CHALMERS
UNIVERSITY OF TECHNOLOGY

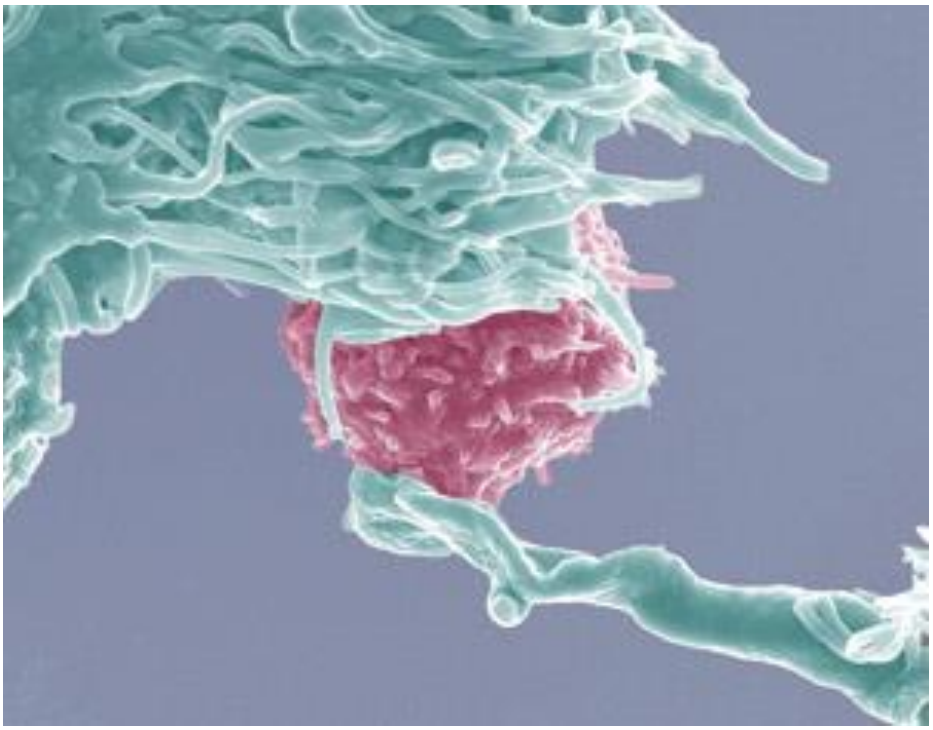

SUPPORTED LIPID BILAYERS DERIVED FROM ANTIGEN PRESENTING CELLS

A SURFACE-BASED APPROACH TO STUDY THE CELL-CELL INTERACTIONS OF THE IMMUNE SYSTEM

Master's Thesis in the Master's Degree Program Biotechnology

ELIN SWANBERG

Supported Lipid Bilayers Derived from Antigen Presenting Cells

A Surface-Based Approach to Study the Cell-cell Interactions of the Immune System

Elin Swanberg

Department of Applied Physics

Division of Biological Physics

Chalmers University of Technology

Gothenburg, Sweden 2016

Supported Lipid Bilayers Derived from Antigen Presenting Cells
A Surface-Based Approach to Study the Cell-cell Interactions of the Immune System
ELIN SWANBERG

Department of Applied Physics
Chalmers University of Technology
SE-412 96 Gothenburg
Sweden

Telephone: + 46 (0)31-772 1000

Printed at Chalmers Reproservice
Gothenburg, Sweden 2016

Cover image by Olivier Schwartz, Virus and Immunity Group, Institut Pasteur, Paris, France
Cell of the month: A dendritic cell sensing a lymphocyte
Published in Nature Cell Biology 6, 188 (2004)

Supported Lipid Bilayers Derived from Antigen Presenting Cells
A Surface-Based Approach to Study the Cell-cell Interactions of the Immune System

Elin Swanberg
Department of Applied Physics
Chalmers University of Technology

ABSTRACT

The cells in our immune system communicate with each other to describe, and warn about dangerous pathogens, as well as to remember and retain protection against diseases we have already had. These functions are dependent on the system of antigen presentation (AP), where reporting cells (for example dendritic cells and B lymphocytes) gather information and present it to the rest of the immune system to initiate a response. This cell-cell contact, also called an immunological synapse, has been previously studied on supported lipid bilayers (SLBs) where the synapse is triggered on artificially constructed membranes intended to mimic the surface of the AP cells, but lacking the transmembrane proteins and mobility of a cellular membrane. In the last year, a new method of producing SLBs has been presented, where the complexity of the cell membrane is retained by use of native membranes, and the mobility and functions of the transmembrane proteins is preserved by fusion with PEGylated synthetic lipid membranes.

The aim of this master's thesis is to derive native membrane vesicles (NMVs) from the membranes of cells of the immune system, and produce SLBs with the purpose of studying cell-cell interactions with the complex composition of natural membranes, using surface sensitive techniques. The primary technique used in this project is total internal reflection fluorescence (TIRF) microscopy, which has been used to study the formations of SLBs, their fluidity, and to detect antibody labeled complexes on the SLBs.

Results from this master's thesis work show formation of SLBs using NMVs. Retained functions of the membranes are seen as the antigen presenting complex (major histocompatibility complex type II) was detected on B lymphocyte derived SLBs. Furthermore, specific interaction between live T lymphocytes and B lymphocyte derived SLBs were observed. The work in this master's thesis therefore supports further use of the presented method to study membrane functions of cells by production of SLBs from NMVs. The results from this project also provides foundation to further study cell-cell interactions and membrane functions of the cells of the immune system using the developed methods.

ACKNOWLEDGEMENTS

I would like to thank my main supervisor and examiner Marta Bally, as she has supported me with a lot of guidance, ideas and great enthusiasm through this project.

I would also like to thank my other supervisors, Karin Norling and Hudson Pace, for all of their help and knowledge. I have very much enjoyed working on my thesis at the department of Biological Physics, and would like to thank the entire group for the fun times and great discussions, both in the lab and during fika breaks.

In addition, I would like to thank Peter Jönsson who has very kindly provided cells to this project, as well as his great knowledge and ideas.

Lastly I would like to thank my amazing friends, family and fiancé for their support through all my years at Chalmers. I would not have made it through these years of hard work without your support.

TABLE OF CONTENT

1 INTRODUCTION

The adapted immune system plays a key role in our defense against diseases and has been of particular interest to humans since the development of the first vaccine. Our body's ability to detect specific antigens and to retain protection against them is a vital function without which humanity would not have survived. These functions of the immune system are based on complex interactions between immune cells, that work together to extend the protection beyond the powerful, but limited, innate immune system.

One of the most essential physiological processes of the innate immune system is the so-called antigen presentation. This is a communication process that takes place between the cells that have first encountered the pathogen, and the rest of the immune system, leading to the initiation of a response specific to the antigen presented. During the process of antigen-presentation, peptides of the pathogen are engulfed by the antigen presenting cell (APC), digested and then presented on the surface of the cell, providing information about the pathogenic attack. This information is further communicated through a number of biomolecular interaction between the surface of the APC and T lymphocytes which leads to the creation of a cell-cell contact, a so-called immunological synapse. The details of this interaction are of great importance for understanding how the immune system works, and how it is all connected.

To facilitate the visualization of cell-cell connections in general, and of the immune synapse in particular, many different methods have been used. A promising one is based on the construction of synthetic supported lipid bilayers (SLBs) acting as simplistic model membranes constructed to mimic the surface of APCs. A major advantage of such constructs is that they facilitate detection and characterization using surface-sensitive techniques. While this method is powerful, it lacks the needed complexity of a native membrane to fully represent the reactions that take place on the cell surface. Using a newly developed method of SLB formation from native membrane vesicles (NMVs) (1), this master's thesis investigates the potential of using NMVs from cells of the immune system to study cell-cell interactions using surface sensitive techniques.

2 THEORETICAL BACKGROUND

2.1 CELLS OF THE ADAPTED IMMUNE SYSTEM

The function of adapted immunity of the body is based on a system of antigen recognition and immunological memory. When a pathogen enters the body, it is recognized by antigen presenting immune cells (APC) that transport the antigen to lymphocytes in the lymphatic system. There, the antigen is presented in a protein complex on the APC surface to the T lymphocytes. (2) This results in a response to the attack, manifested by a release of subsets of signals to other immune cells depending on the pathogen, but also in the creation of memory lymphocytes that allow for a quicker response if the same pathogen is to be discovered again. (3)

There are different types of APCs categorized as macrophages, B lymphocytes and dendritic cells, where the last two have been used in this project together with T lymphocytes. The functions of these cell types are described below, as well as the specific cell lines used in this project.

2.1.1 Dendritic cells

Dendritic cells (DCs), also called Langerhans, are a type of APC found in tissues all over the body. They are positioned under barriers of epithelial cells and continuously sample the extracellular fluid for pathogens. The DCs become activated by signals released from other immune cells, like macrophages and neutrophils. They can also be activated by their pattern recognition receptors that recognize a broad spectrum of pathogens. At the point of activation, the DC retains a sample of a stimulating pathogenic antigen and then travels through the lymphatic system to the nearest lymph node. (3) As the activated DC matures, it loads the antigen peptide onto the major histocompatibility complex (MHC) class II, to be displayed on the cell surface and further presented to T cells leading to formation of an immunological synapse. When the DC reaches the lymph node it only survives there for a few days, thus providing a time limited “snapshot” for the responding T cells. (3)

In this project the D1 cell line of dendritic cells was used.

2.1.2 B lymphocytes

B cells are APCs utilized in later stages of a pathogenic attack. They are not potent for T cell activation in their initial non-activated state, the initial response and antigen presentation is therefore performed by DCs. However, in the event of a longer ongoing infection, or on the occasion of the return of the same pathogen, B cells act as effective responders. B cells are activated by readily activated T cells, through complex formation which then leads to further activation of naïve T cells by the B cells. (3)

Compared to other APCs, B cells are highly efficient at collecting and concentrating the peptides. This is due to the fact that the B cell receptors which recognize the antigen, interacts with very high affinity with the antigen thanks to its antibody-like construction. This high affinity to antigen provides potential for a very high MHC presentation density on the surface, and therefore a very high T cell activation potential. A threshold number of T cell receptors is required to cluster in order to activate the T cell. With the higher level of presentation of antigen in B cells it is therefore estimated

that they hold a 100- to 10 000-fold advantage over other APCs as a low number of B cells can create the required level of clustering to activate the T cell. (3)

The B lymphocyte Raji cell line is used throughout this project.

2.1.3 T lymphocytes

Although they are not APCs, T cells and B cells are very similar in appearance, as they both have a round morphology and grow in the bone marrow. The T cell receptors (TCR) are, similarly to B cell receptors, very specific in their recognition capability. The TCR is used to connect cells to the antigen presentation of other cells, leading to the formation of a synapse, and therefore to a response to the pathogen, if the pathogenic peptide is properly presented. Upon activation, the T cell proliferates, leading to the accumulation of T cells of the relevant specificity, a process which increases the defensive force. (2)

There are three major groups of T lymphocytes with separate functions. Killer T cells attack the body's own cells after viruses have infected them. They recognize problems in the cells by scanning peptide presentation on the cell surface in MHC type I, which specializes in presenting proteins produced inside the cell. Almost all cell types in the body present MHC type I on their membrane as a constant update on the ongoing processes of the cell. Upon discovery of a virus infection, the killer T cells induce apoptosis in the infected cells to inhibit spreading of the virus. (2) Regulatory T cells protect the immune system from harmful overreactions to pathogenic stimuli (3). Helper T cells are activated through antigen presentation by MHC type II on APCs, and create a specific response by secretion of cytokines. These cells which take part in the immunological synapse are the type of T cells that are used in this project.

The cell line used in this project is the T lymphocyte Jurkat, which is a helper T cell.

2.1.4 Antigen presentation and synapse formation

As previously described, class I MHC is a complex that is displayed on most cell types in the body to provide information on ongoing cellular processes. The class II MHC complex works in a similar way and exhibits an analogous structure of peptide presentation. However, in contrast to MHC class I, class II proteins only mediate the presentation of antigens collected from pathogens from the surrounding environment on APCs. In this case, the detected pathogenic proteins are taken up, digested and loaded onto the MHC inside the cell before presentation. The biggest structural differences between the two types of MHC are that class I contains one large chain that stretches through the membrane, combined with a smaller protein. The class II complex contains two large protein chains (α and β), which both stretch through the membrane. Because of this difference in structure, the class II complexes can carry larger antigen peptides than class I complexes, usually around 20 amino acids long.

Another specific function of the APCs is to provide co-stimulation, which is required in addition to the MHC presentation to activate T cells. APCs therefore in reality refers to cells that provide both MHC class II complexes as well as other co-stimulatory proteins, in addition to the ubiquitous MHC class I. The co-stimulatory activation interaction often includes B7 on the APC and connecting CD28 on the T cell. (3)

T cells express either CD4 proteins, if they are helper cells, or CD8 proteins, if they are killer cells. These proteins aid in attaching to the MHC at the beginning of synapse

formation. They are also involved in strengthening the downstream signaling into the cell to initiate activation. The TCR in turn connects to a larger complex of proteins in the membrane, called CD3. These proteins are anchored in the membrane but extend into the cytoplasm and relay the signals from the TCR connection. (2) The cell-cell connection between an APC and a T cell is visualized in a simplified manner below in figure 1.

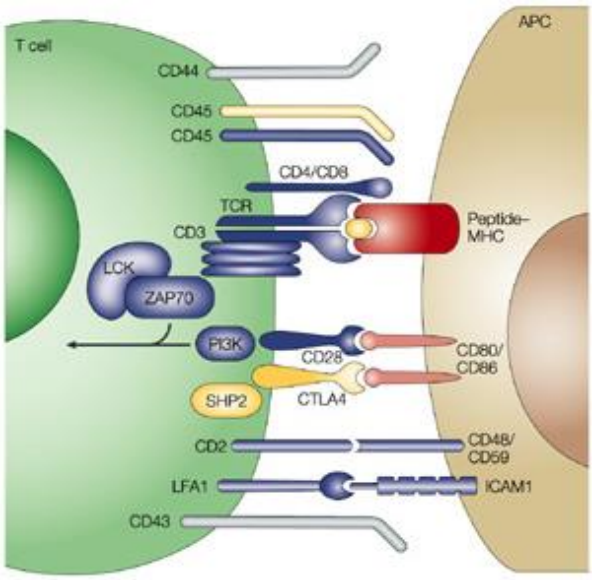

Figure 1 Formation of an immunological synapse between an APC and a T cell, picture from (4).

The immunological synapse forms in the arrangement of a bull's eye consisting of supramolecular activation clusters (SMACs). These structures start forming after a few minutes of cell-cell contact. The central area of the SMAC arrangement consists of the TCR and MHC peptide complexes which are then surrounded by a ring of integrin LFA-1, interacting with ICAM-1. The formation of the synapse is dependent on a functional T cell cytoskeleton, and occurs in a series of temporal stages: T cell polarization, initial adhesion, synapse formation and synapse maturation. (5) Formation of SMAC rings results in movement and separation of the membrane components according to the kinetic segregation model. This model explains the changes in kinase and phosphatase activity that take place during the formation of the synapse. During the cluster formation, larger membrane structures, such as the CD45, are excluded from the innermost area, as they are larger than the distance between the membranes. During normal conditions, when no synapse is formed, there is an ongoing equilibrium between kinases and CD45 to keep an overall low TCR-CD3-complex phosphorylation. When the CD45 is sterically excluded from the sight of the synapse, the equilibrium is disrupted, resulting in TCR phosphorylation by tyrosine kinase. This allows for recruitment of ZAP-70, and the activation of downstream signaling pathways in the T cell. (6)

2.2 CELLULAR MEMBRANES

The following section describes the structure, components and functions of cellular membranes. Models for studying membranes in the form of supported lipid bilayers

(SLBs) are also described, as well as previous work using SLBs to study the membrane components and interactions of the immune system.

2.2.1 Cell membranes

The membranes of cells are envelopes that separate and shield the cellular components from the surrounding environment. As shown in figure 2 the structure of a cellular membrane is based on a two leveled sheet of ordered lipid molecules which further carry a variety of embedded and anchored biomolecules. Together, they form a complex and fluid mosaic which fulfils crucial functions for the cells survival, in particular by mediating transport and signaling processes. Membranes exhibit a high degree of spatial heterogeneity. They include patches of different compositions, for example lipid rafts, where the lipids are packed more tightly in presence of cholesterol, resulting in clustering of different protein types. (5) As a result of this heterogeneity different areas of the membrane vary in their thickness and overall protein content. Another important feature of the cell membranes is their asymmetry (i.e. the inner and outer leaflets have different compositions) which is crucial in the context of cell communication or membrane fusion. (7) The complexity of the reactions and functions of these dynamic materials is difficult to mimic, but important to study in order to understand many basic functions of cells.

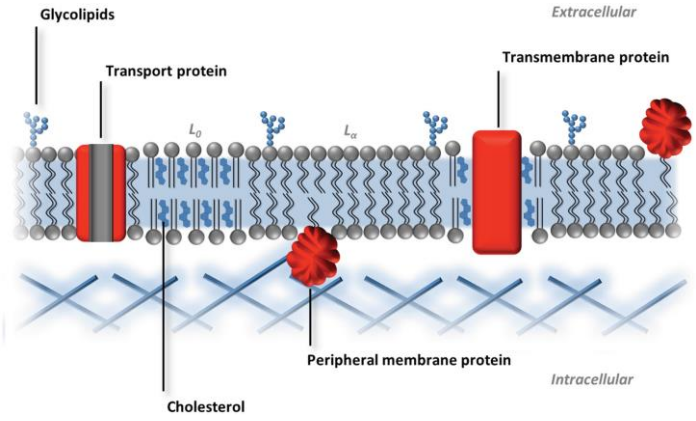

Figure 2 Illustration of a native cell membrane, picture adapted from (7)

2.2.2 Model supported lipid bilayers

SLBs, formed on glass surfaces, are a useful model system to investigate the characteristics of molecular interactions taking place in adhesive cell contacts (8). A SLB is a constructed planar membrane, assembled in vitro and sitting on a solid support. SLBs work as a model for investigating the functions of the cell membrane, as they are homologous in their structure to their native counterpart (1).

The SLB model is widely used to study different molecular interactions and cell-cell contacts as it provides several advantages, such as stability of the bilayer, a control of the composition as well as the possibility of imaging the interfaces with surface-sensitive techniques (4). Furthermore, the functional components of the membrane are better studied in environments that are more representative of their native state, as well as retain the lateral mobility of a lipid structure. Nevertheless, SLBs are often simplified

models compared to the cell membrane, and do not completely represent the complexity of real membranes. They are often constructed from only a few constituents, mostly lipids only. As a result, the SLB model does not have the activity of a native membrane, as it often doesn't contain transmembrane proteins. Furthermore, the mobility of the components that are present in a cellular membrane may not be preserved. Nevertheless, simplistic versions of model membranes are an interesting platform for mimicking cell-cell interactions and other membrane functions.

One common method to produce SLBs is by the LB/LS technique (Langmuir-Blodgett/Langmuir-Schäfer) where a lipid monolayer is formed on a water surface with an organic solvent by evaporation. A hydrophilic substrate is then submerged and slowly lifted while under constant pressure, making the monolayer stick to the sample surface. (7) Another common method to form SLBs is by production of lipid vesicles or proteoliposomes that interact with a hard surface, under specific conditions, to rupture and form a layer. (7) This is the method utilized in this master's thesis. The SLB formation takes place in 2 steps: the vesicles first adsorb to the surface before starting to rupture, catalyzing further bilayer formation and leading to the formation of a larger continuous SLB from the smaller bilayer patches. (9) This process is illustrated in figure 3.

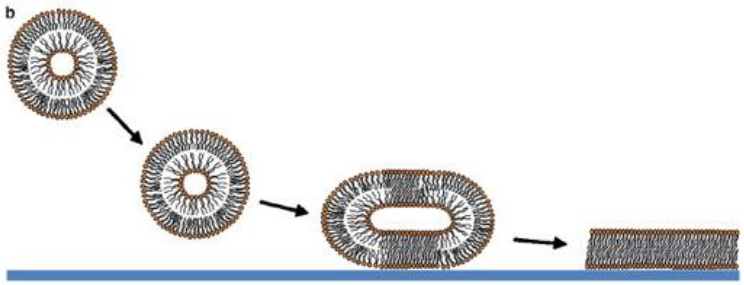

Figure 3 Illustration of the formation of a SLB by rupture of lipid vesicles. Picture adapted from (10)

Silica-based materials, like glass, mica and SiO_2 have been traditionally used as substrates for SLB formation, as they permit microscopy-based observation and facilitate vesicle rupture. Nowadays other materials are used as well, like PDMS (polydimethylsiloxane), titanium, alumina and gold. The latter has enabled the use of SPR in the study of SLBs. (7)

Cushioned SLBs have been developed in order to suspend the SLBs over the substrate surface, improving the lateral mobility of components of the model membrane and facilitating the study of large transmembrane protein structures. (9) This is illustrated below in figure 4. A commonly used molecule for cushioning is poly(ethylene glycol) (PEG). (9)

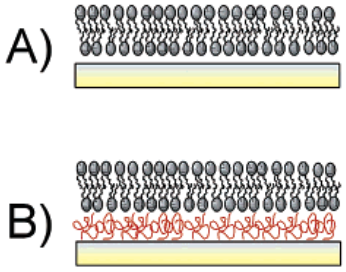

Figure 4 Illustration of a SLB (A) and a cushioned SLB (B). Picture adapted from (9)

2.2.3 Previous use of supported lipid bilayers to study immunological cells

SLBs have been used extensively in order to study the interactions governing cell-cell communication for the immune system. Many different systems have been created using synthetic model membranes, with functional biomolecules incorporated, in order to initiate a response from other immunological components, and study the reactions. (8) One example from the 80s is the formation of FC receptor systems, where antibodies were attached to SLBs and engaged with live macrophages (11).

In order to study the major histocompatibility complex (MHC) of antigen presentation, the MHCs were purified and incorporated into synthetic SLBs by liposome fusion in the beginning of the 80s. With this platform, different types of T lymphocytes were activated upon contact. As the complex structure of the synapse was less known then, it was done to investigate the function of antigen presentation. At the time, it was successfully demonstrated that the MHC interacts with the TC receptor, using a peptide from the pathogenic antigen. (12)

To further investigate the specific interactions occurring on cell surfaces, specific components, suspected to be involved in adhesion, were used in the experiments. CD45 was reconstituted in SLBs and used to demonstrate the interaction with CD2. SLB models later made it possible to investigate the molecular segregation that occurs during synapse formation. (8)

In 1996 it was found that larger transmembrane proteins are laterally immobile in a SLB because the domains between the membrane and the underlying substrate are trapped. This was shown by comparing two versions of CD58 where one type was larger and had a transmembrane structure, leaving it completely immobile, while still retaining its binding properties. In contrast the other CD 58 form was highly mobile in the upper leaflet of the bilayer. (13) The reason for changes in mobility for labeled proteins was attributed to defects in the bilayer and proteins interacting with or being trapped against the glass substrate. Furthermore, it was concluded that high levels of proteins in the liposomes were problematic as they interfered with the formation of SLBs. To overcome this problem, the material was diluted with liposomes to produce predictable protein densities and achieve SLB formation. (8) At that time, it was believed that the density of free ligands inside the contact area was approximately equal to surrounding the contact area (8). In 2001 it was shown that the density of free molecules in the contact area is less than in the surrounding bilayer, by labeling of different molecules of

the bilayer (14). The conclusion was drawn that exclusion occurred because of the cellular glycocalyx. The possibility of measuring 2D affinity and kinetic rates of the bilayer facilitated investigations of the biomolecular interactions that take place in contact areas. This early structural knowledge suggested and led to the understanding that T cell adhesion in cell-cell contact requires segregation between membrane components, a process regulated by the size of different biomolecules. (8) The proof of segregation in synapse formation was provided using both cell-bilayer and cell-cell interaction studies in the late 90s, when segregation was shown to occur both thanks to passive and active cellular processes. (15) The molecules were later proven to not only separate but reorganize in circular clustering structures with MHC-TCR accumulation in the center. (16)

SLBs as a platform for studying the immunological synapse have given a lot of information and insight into the functions and communication of the immune system. They have made it possible to identify ligands of importance for activation of pathways, to investigate the reactions that take place in adhesion between cells, and to visualize the formation of the synapse. There are still many questions to be answered, and SLB systems will continue to provide new answers as the technique develops further. The most important aspect of the SLB technology is the ability to collect highly quantitative data on the cell-cell interface. (17)

2.2.4 Previous work with supported lipid bilayers derived from native membranes

The methods used in this thesis project to produce SLBs from NMVs are based on previous work with NMVs at Chalmers University of technology. As previously mentioned, a protocol for the formation of SLBs from NMVs was developed and published in 2015 (1). The following text will shortly describe the study. In addition, an alternative approach to produce SLBs from native membranes of complex composition, published in 2016 (18), developed in the United States, will be described. The latter method was not utilized in this project.

In the protocol developed at Chalmers (1), the NMVs were produced through a procedure where cells were lysed and the membrane material was collected by ultra-centrifugation. BACE1 containing Baculovirus NMVs were merged with PEGylated synthetic POPC vesicles using bath sonication. The hybrids were then allowed to rupture onto a hard surface to form a polymer-supported lipid bilayer. The procedure is summarized below in figure 5.

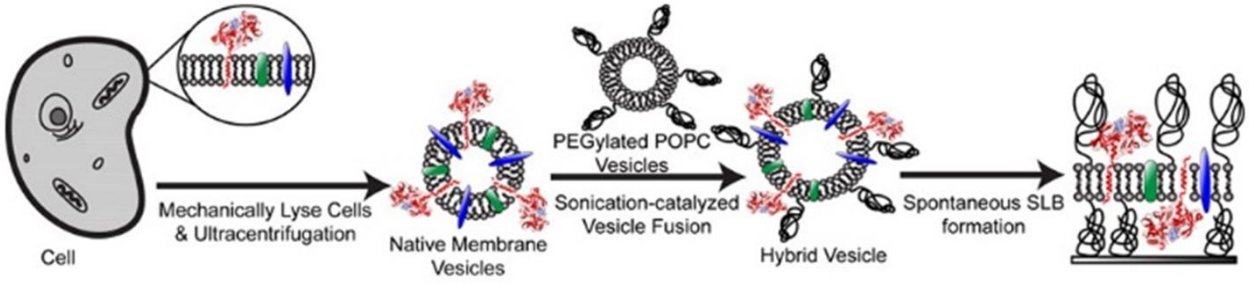

Figure 5 Procedure of SLB formation from native membrane material. Picture from (1).

An alternative method of producing SLBs from native membrane material was suggested in the publication from 2016 (18), where cell blebs were used as an intermediate in the production of cushioned SLBs. In contrast to the previously described study, this procedure allows the protein orientations of the native membrane to be retained through the procedure, as the blebs are not ruptured by sonication. The SLB formation occurs in a "parachute mechanism", allowing the membrane components to keep their orientation. This study was performed using HeLa cells, which were treated with serum starvation or chemical induction to induce blebbing. This procedure is visualized below in figure 6.

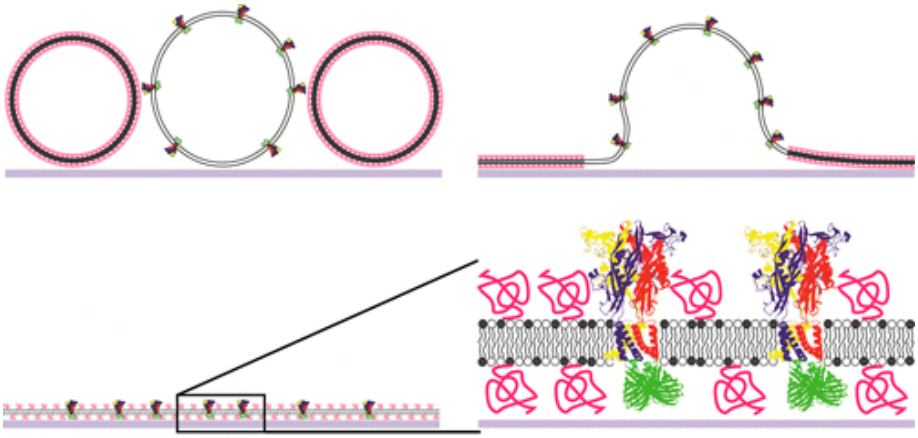

Figure 6 Rupture of cell blebs with PEGylated lipid vesicles. Picture from (18).

2.3 TECHNIQUES USED

The following section will describe the techniques used for the experiments performed in this project. Theoretical background will be provided regarding Total Internal Reflection Fluorescence Microscopy (TIRF), Fluorescent Recovery after Photobleaching (FRAP) and Fluorescence Resonance Energy Transfer (FRET).

2.3.1 Total internal reflection fluorescence microscopy

TIRF microscopy is a method that enables detection of fluorescence in a very thin region of a sample. The technique, which can be used in both aqueous and cellular environments, excites fluorophores situated just above the sample surface in a region approximatively 100 nm thick. The excited thin section is called an evanescent field and decays exponentially as the distance from the investigated interface increases. (19) Because the surrounding bulk sample is not illuminated, the method is characterized by very low background noise in the resulting images. The evanescent field

TIRF microscopy is based on illuminating a glass surface at high incidence leading to total internal reflection of the illumination light. This reflection generates the evanescent field which has the same frequency as the incident light. (19) The minimal angle required for the beam to reflect is called the critical angle, and is calculated from

$$\theta = sin^{-1}\left(\frac{n_1}{n_2}\right)$$

Where n_1 and n_2 are refractive indices of the liquid and the solid. The intensity of the evanescent field for an infinitely wide beam is calculated as

$$I(z) = I(0) \cdot e^{\frac{-z}{d}}$$

Where

$$d = \frac{\lambda_0}{4\pi}(n_2^2 sin^2\theta - n_1^2)^{\frac{-1}{2}}$$

Therefore, the intensity decreases with the distance from the interface, z. λ_0 is the wavelength of the incident light in vacuum. d is the depth and decreases with increasing angle. (19)

2.3.2 Fluorescence recovery after photobleaching

Fluorescence recovery after photobleaching (FRAP) is a method to determine the diffusion and mobility of a biological molecules. To perform FRAP, a high intensity laser pulse is applied to a specific point of the sample. This causes photobleaching of the fluorescent molecules that are hit by the laser, after which the recovery of fluorescence in the area of impact can be observed. Fluorescent molecules in the surrounding area will diffuse into the bleached spot, creating an influx of intensity that can be detected and analyzed. (20)

Quantitative information of the transport of molecules can be extracted from the time evolution of the recovery, using different calculation models. There has been a variety of FRAP calculation models developed, that can be applied for specific conditions. A simple way to describe the recovery of the bleached spot mathematically is with an exponential function:

$$\frac{F(t)}{F_0} = 1 - be^{\frac{-t}{\tau}}$$

Where F_0 is the initial fluorescence intensity, and F(t) is fluorescence in the bleached spot at the time t. τ is characteristic recovery time and related to halftime of recovery by

$$\tau = \frac{t_{\frac{1}{2}}}{ln2}$$

And b is the fraction of fluorophores that are bleached.

From the exponential recovery curve, information can be gained about the rate of diffusion, but these calculations can only be used in relative comparison for experiments performed using the same settings, as the t ½ time is dependent on the size of the bleach spot etc.

It is also possible to estimate the diffusion from the recovery halftime using

$$D = \gamma\left(\frac{w^2}{4t_{\frac{1}{2}}}\right)$$

where γ is a correction constant that is dependent on the bleaching area and amount of photobleaching. w is size of bleached area. (20)

2.3.3 Fluorescence resonance energy transfer

Fluorescence resonance energy transfer (FRET) is a method to measure the proximity of two molecules in a sample. The method requires a donor fluorophore in an excited state that transfers its excitation energy to a nearby acceptor. In order for FRET to occur there has therefore to be an overlap between the emission spectra and absorption spectra of the donor and the acceptor group respectively. This is illustrated below in figure 7. (21) The transfer of energy quenches the donor fluorescence, and increases the emission of the accepting group a process that can be detected with a fluorometer.

Theodor Förster described the rate of energy transfer between the two groups with the equation:

$$K_T = \left(\frac{1}{\tau_D}\right) \cdot \left[\frac{R_0}{r}\right]^6$$

Where R_0 is the Förster critical distance and r is the distance separating the two. τ_D is the donor lifetime without the presence of the acceptor. As seen in the equation, the energy transfer efficiency decreases at the power of six of the distance. This gives a total range of approximately 10 nm for FRET to take place. (22) The reaction is dependent on the lifespan of the donor fluorescence to be long enough for the transfer to take place.

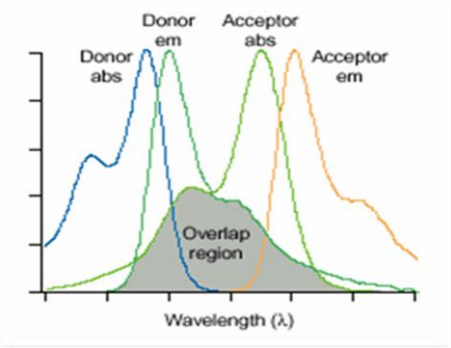

Figure 7 Illustration of the absorption and emission spectra for the donor and acceptor groups in a FRET assay. Picture adapted from (21)

FRET can be used to gain structural information about the placement of donor- acceptor pairs in a sample. (22) This is visualized in the example of the image below (Figure 8) where FRET is used to detect the interaction of two proteins by monitoring the emission intensity from the acceptor group upon close proximity.

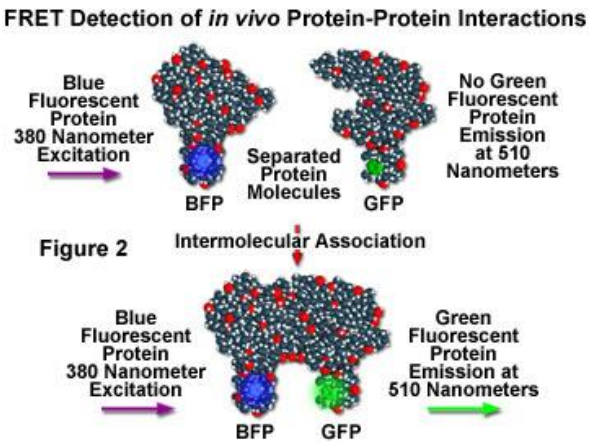

Figure 8 FRET detection, visualized example. Picture from (22)

The possibility to determine the distance between the probes makes FRET also a useful method to determine fusion of lipid vesicles. In a lipid-mixing assay, membrane material is labeled with a combination of the donor and acceptor lipid probes. When the labeled lipids are mixed with unlabeled membrane material FRET decreases due to the increased separation of the probes and accordingly and increased donor fluorescence intensity and a decreased acceptor fluorescence can be observed (Figure 9). This lipid mixing assay was utilized in the project where vesicles containing rhodamine (acceptor) and NBD (donor) lipids were fused with NMV material. FRET between NBD and rhodamine outputs a rhodamine emission at 585 nm from a NBD excitation at 470 nm.

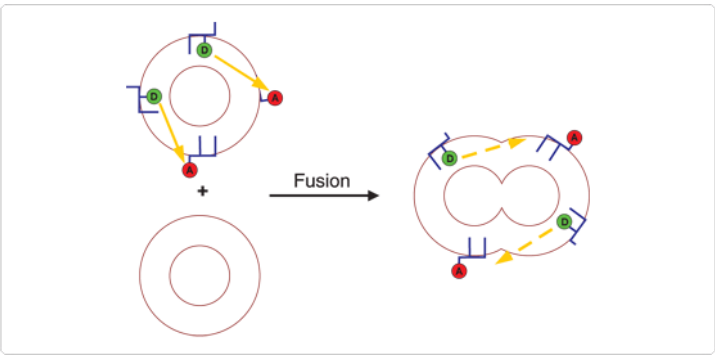

Figure 7 FRET between rhodamine and NBD fluorescent groups during mixing of lipid vesicles. Picture from (23)

3 AIM

The aim of this master's thesis is to derive and characterize native membrane vesicles (NMVs) from the membranes of cells of the immune system, which are relevant for the formation of the immunological synapse. These NMVs are then used to produce supported lipid bilayers (SLBs) from the formed NMVs which are further characterized. Furthermore, the project aims at investigating the potential of a native-like SLB to study cell-cell interactions. The advantage of this method is that the complex composition of natural membranes is preserved and that surface sensitive techniques can be used to visualize the cell-cell interactions and specific components of the membrane.

4 METHODS AND MATERIALS

4.1 OVERVIEW

In this project, three different cell types where used: Jurkat cell line (T lymphocytes), Raji cell line (B lymphocytes) and D1 cell line (dendritic cells). These cells where homogenized and centrifuged (protocol described below) to extract the membrane materials of the cells and remove all other cell components. The native membrane vesicles (NMVs) that remain after the procedure where then frozen.

NMV material was mixed with synthetic PEGylated 1-palmitoyl-2-oleoyl-sn-glycero-3-phosphocholine (POPC) (PEG_POPC) vesicles and fused into hybrids by bath sonication. The NMVs and hybrid vesicles where then characterized and used to form SLBs. The biomolecular content and functionality of the bilayers was further investigated in cell experiments assessing the interaction between the bilayers and live immunological cells.

4.2 CELL CULTURE

D1 cell line, kindly provided by Professor Nils Lycke at Sahlgrenska University Hospital, was used for the preparation of NMVs immediately upon delivery. The D1 cells were stimulated with lipopolysaccharides (LPS) at 10 µg/ml 24 hours before transport, to trigger antigen presentation by the cells.

Raji and Jurkat cell lines, kindly provided by Peter Jönsson at Lund University, were cultured at 37°C and 5 % CO2 in RPMI-1640 medium (Sigma Life Science) supplemented with 10 % inactivated fetal bovine serum, L-glutamine, sodium pyruvate, Penicillin-Streptomycin-Neomycin and HEPES (4-(2-hydroxyethyl)-1-piperazineethanesulfonic acid).

4.3 PREPARATION OF NATIVE MEMBRANE VESICLES

Cells were first washed with homogenization buffer, consisting of 2xPBS (phosphate buffered saline, tablets) and protease inhibitor cocktail (Roche Life science, tablets). In the case of D1 cells, the cells were collected off the plates, using cell scrapers (BD Falcon). In the case of Raji and Jurkat cells (cell suspensions) the cells were centrifuged (410xg, 5 min, Hettich Mikro 22R), and the pellet resuspended in 3 mL to remove the growth media.

All cells were centrifuged and resuspended in 3 mL three times (5 min, 1000xg, 4°C) in order to wash the cells. The cells were then homogenized using a Dounce Homogenizer with a tight fitting pestle (40 strokes). The solution was centrifuged (600xg, 5 min) after the homogenization, and homogenized again. This process was repeated until no pellet was collected in the centrifugation step.

To remove the nuclei and mitochondria from the lysed cell solution, the sample was centrifuged (3500xg, 20 min). The remaining supernatant was then centrifuged in an ultra-centrifuge at 180 000xg (Optima LE-8K, Beckman Coulter), at 4°C for 90 minutes to collect the membrane material. The collected pellet was resuspended in storage buffer (2xPBS, 20%vol glycerol) to give an approximate concentration of 10 mg/ml, based on the pellet weight. The aliquots were then frozen using N_2(l), and stored at -80 °C.

4.4 SONICATION CONDITIONS AND FUSION POTENTIAL

To investigate the potential of the NMVs to fuse into hybrids with synthetic vesicles, the mixing was investigated using FRET. To gain the optimum conditions for fusion, different conditions for bath sonication were tested for all types of NMVs.

To carry out such experiments, FRET vesicles consisting of 1 mol % Lissamine rhodamine B- 1,2-dioleoyl-sn-glycero-3-phosphoethanolamine (LRB-DOPE), 1 mol % NBD-DOPE, 98 mol % POPC, (extruded through a 100nm membrane), provided by Dr. Hudson Pace, were used. 1 µL of these vesicles (1mg/mL) was added to thawed NMV solutions (5 µL in the case of D1 derived NMVs, 20µL in the case of Raji and Jurkat derived NMVs) that were then further diluted with PBS to a total volume of 60 µL. The samples were bath sonicated (except control) and following conditions were investigated: Temperature 30 °C or 35 °C; sonication time: 5 min or 10 min. After sonication, the samples were diluted with MilliQ water to a total volume of 300 µL and analyzed in a fluorometer (Photon Technology International). Emission scans were acquired between 490 nm and 650 nm, with three readings per sample. All samples were run in duplicate and the results are presented as averages of the two.

4.5 CHARACTERIZATION OF NATIVE MEMBRANE VESICLES

The NMVs were investigated in order to quantify their phospholipid content, protein content and to estimate the total membrane material of the vesicles.

The phospholipid content was determined by using a phospholipid assay kit (MAK122, Sigma-Aldrich), where the total fluorescence is detected by plate reader (FLUOstar OPTIMA microplate reader, BMG Labtech, Germany) and compared to a standard curve prepared together with the samples.

The protein concentration was determined with a CBQCA Protein Quantitation kit (C-6667, Molecular Probes). The assay was kindly performed by Karin Norling, PhD Student at Biological Physics, Chalmers.

To estimate the material content, the results from the previously described FRET assay (section 4.4) were used, as the ratio of the peaks depend on the FRET probes, and thereby the amount of material that is mixed between them. The calculation to estimate the concentration of materials was done by comparing the peak ratio (590/530nm) from the FRET experiment carried out with NMVs with the values of a calibration curve obtained by mixing POPC vesicles of known concentrations and, containing the same FRET probes at the same concentration. The slope of the calibration curve gives therefore the estimated concentration of POPC vesicles needed to produce the same FRET signal. Note that the estimation of the total membrane material using the FRET-based assay is dependent on the assumption that the sonication is optimal and all material is mixing. Furthermore, the estimation is done based on the molecular weight of the much simpler structured POPC vesicles, providing therefore a concentration in "POPC equivalents". As the composition of the native cellular membrane is more complex, the estimation mostly provides a relative measurement between the samples.

4.6 FLUORESCENCE MICROSCOPY

All fluorescence microscopy experiments were carried out using an epifluorescence micoroscope equipped with a TIRF setup (Inverted Nicon Eclipse Ti-E microscope, Nikon Corporation, Japan), a 60x objective and equipped with a camera (Andor Ixon+, Andor Technology, Ireland). FRAP was performed with a green laser (diode pumped solid-state 532 nm laser from B&W TEK Inc. with a 100 mW output).

4.7 SUPPORTED LIPID BILAYER FORMATION

Bilayers were formed, in the following experiments, using different volume percentages of NMVs to PEG_POPC. The PEG_POPC vesicles containing 0.5 mol % PEG5000-ceremide, 99.5 mol % 1-palmitoyl-2-oleoyl-sn-glycero-3-phosphocholine were provided by Dr. Hudson Pace.

Table 1 Mixing compositions of NMV hybrid vesicles.

NMV percentage	Volume NMVs	**Volume PEG_POPC (1mg/mL)**	Volume PBS
10%	3uL	27uL	30uL
20%	6uL	24uL	30uL
30%	9uL	21uL	30uL
40%	12uL	18uL	30uL

The hybrid mixtures were prepared according to table 1, and then bath sonicated for ten minutes at 30°C for D1 and Raji NMVs, or at 35°C for Jurkat NMV hybrid formation

The bilayers were formed by addition of sample to clean glass substrates (cover glass, 24x40 mm, 0,13 - 0,17 mm thick) that had been previously boiled in diluted 7X cleaning solution (MP Biomedicals) and rinsed in SDS (sodium dodecyl sulfate,10mM) and MilliQ water. The bilayer formation was contained in wells of a PDMS (polydimethylsiloxane) elastomer, produced in house, that had been placed on the glass substrate. As the quality of the bilayer formed is heavily dependent on the cleanliness of the substrate, each substrate glass slide was tested by formation of a fluorescent, synthetic lipid bilayer of Rho_POPC (0,5 mg/ml, 1 mol% LRB-DOPE with POPC) in one PDMS well before the NMV bilayers were formed.

4.7.1 Supported lipid bilayer formation with tracer vesicles

Tracer vesicles were used in order to investigate the effect of higher levels of native components on the propensity of the hybrid vesicles to rupture and form a bilayer, and to verify bilayer formation by fluorescence microscopy. The fused NMV-hybrids (6uL) were mixed with rhodamine tracer vesicles containing 1 mol% LRB-DOPE, 98.5 mol % POPC (Rho_POPC) (2µL of 0,5 mg/mL) and diluted further with PBS (12µL) to reach a total volume of 20µL. 8 µL of sample was added per well for bilayer formation.

The tracer rhodamine-containing vesicles serve as a visual detection of individual vesicles landing on the substrate, and make the rupture events visible as the bilayer is formed by a large rupture event started by several smaller events. The tracer vesicles

are visible as they are fluorescent and land on the substrate surface, and disappear as they rupture together with the surrounding NMV hybrid vesicles to form the bilayer.

The fluorescence of the tracer vesicles during the formation of the bilayers was detected using the TIRF microscope (see section 4.6). Time lapse movies were acquired at 1 frame per 5 seconds. The addition of hybrid-tracer solution to the PDMS well, for bilayer formation, was done between frames in order to detect the process from start.

The data was evaluated using an in house detection software (MATLAB) where thresholds are set for the fluorescence required for detection as vesicles. Set thresholds that are displayed in the results are set to high = 800, medium = 200 and low = 200.

4.7.2 FRAP with rhodamine labeled D1 hybrid bilayers

In order to investigate the diffusion properties of the lipids in the fluid bilayer, D1 NMVs were mixed and sonicated with PEG_POPC vesicles labeled with rhodamine markers in different volume compositions (Rho_POPC, 1% LRB-DOPE with POPC, 1mg/ml) to create fluorescent hybrid vesicles. The 20% and 30% volume compositions were mixed according to table 1. The mixtures were sonicated, and bilayers formed, according to the procedure described above in section 4.7. The sample was incubated for 2 hours during SLB formation, and rinsed with PBS before detection.

The bilayers were visualized using the TIRF microscope and camera described in section 4.6. For FRAP, bleaching was performed with a green laser (see section 4.6). After bleaching, time lapse movies were acquired at 1 frame per 5 seconds. The movies captured were analyzed using an in house FRAP evaluation software (MATLAB).

4.7.3 FRAP with antibody staining of MHC type II on Raji hybrid bilayers

In order to detect the presence of MHC type II, antigen presenting complexes, on the fluidic bilayer produced by NMVs, Raji NMVs were mixed with PEG_POPC vesicles, provided by Dr. Hudson Pace. SLBs were formed according to the procedure described in section 4.7. Raji NMV solution was mixed with the synthetic vesicle solution at 30% volume compositions, according to table 1. The same was done with Jurkat NMVs to be used as control surface. 8µL of sample was added per well. The samples were incubated for 30 minutes during SLB formation, and rinsed with PBS. The sample volume of each well was then slightly decreased to approximately 5 µl. Thereafter, the samples were incubated with the fluorescent PE labeled anti-human HLA-DR antibody (clone L243, Biolegend). The wells were covered with 5 µL antibody solution at 20µg/mL , added to the sample solution containing the formed SLBs in the wells, and incubated in darkness on ice, for another 30 minutes. The wells were rinsed before imaging and the formed bilayers were investigated by fluorescence FRAP.

The bilayers were visualized using the TIRF microscope, green laser and camera described in section 4.6. with 2 a seconds bleaching and 2 minutes between frames captured. The movies captured were analyzed using an in house FRAP evaluation software (MATLAB).

4.7.4 Bilayer - live cell interactions

NMV solutions from Raji and Jurkat cells were mixed with PEG_POPC solutions to create 30% volume composition hybrids, according to table 1. The mixtures where then further diluted with PBS and sonicated, and bilayers were formed according to the procedure in 4.6, except for a large addition of sample to each well of 60µL, or 120µL, depending on the size of the well. Two well sizes were used, of approximately 80 and 150 µL total volume each.

Bilayers were formed from the Raji hybrids, as well as the Jurkat hybrid solution as control. In addition, bilayers were also formed by non-sonicated, pure PEG_POPC vesicles (0,5 mg/ml in PBS, 0,5% PEG with POPC, 100nm vesicles).

The bilayers were formed during incubation for 30-35 minutes at room temperature and then rinsed with PBS. The liquid volume of each well was decreased to approximately 20 (small wells) or 40 µL (large wells) before addition of cell solution, depending on well size. Live Jurkat cells in culture solution were counted to determine approximate cell concentration. 30µL of cell solution of approximately one million cells per mL was added to each small well and 50 µL to each large well. 30 and 50 µL of media was also added to the wells to maintain good environmental conditions for the cells, resulting in approximately 80 µL total volume in small wells and 140 µL in large wells. Cell suspension was also added to a well of only glass substrate, as an additional control. The cells on SLBs were incubated for one hour in 37^{o}C. Cells were then observed and photographed using a light microscope (DM4000 M, Leica) and 10x objective. Slides with cells were shaken, and additional photos were captured. The wells were then rinsed with medium (10x 40 or 60 µL) before more images were captured. The images are randomly taken of the different types of bilayers after rinsing of the wells. Additional photos were also taken using the fluorescence microscope described in section 4.6, with 60x objective to provide more detailed information on cell morphology.

5 RESULTS

The following text describes the results of the experiments conducted during this project starting with characterization of the formed NMVs and SLBs, and then investigations of native membrane functionality. For each section the results for each cell types are presented.

5.1 CHARACTERIZATION OF NATIVE MEMBRANE VESICLES

As described in methods, the compositions of the NMVs from the different cell types were investigated. The results are summarized below in table 2 for the detected protein content, phospholipid content and the estimated membrane material, determined from the FRET mixing assay. The content of protein and estimated membrane material is seen below in figures 10 and 11, while the ratio of proteins by the estimated membrane material is plotted below in figure 12.

Table 2 Composition of NMV material and ratio of protein to material.

NMVs	Protein Content (mg/mL)	Estimated Membrane Material (mg/mL)	Estimated Membrane Material (uM)	Phospholipid Content (uM)	Phospholipid Content (mg/mL)	Mass Ratio (Protein Content/Estimated Membrane Material)
D1	0,94	0,34	0,48	85,14	0,051	2,75
Raji	0,14	0,076	0,11	-	-	1,85
Jurkat	0,21	0,16	0,23	-	-	1,33
GMK	1,05	0,48	0,67	98,58	0,059	2,20

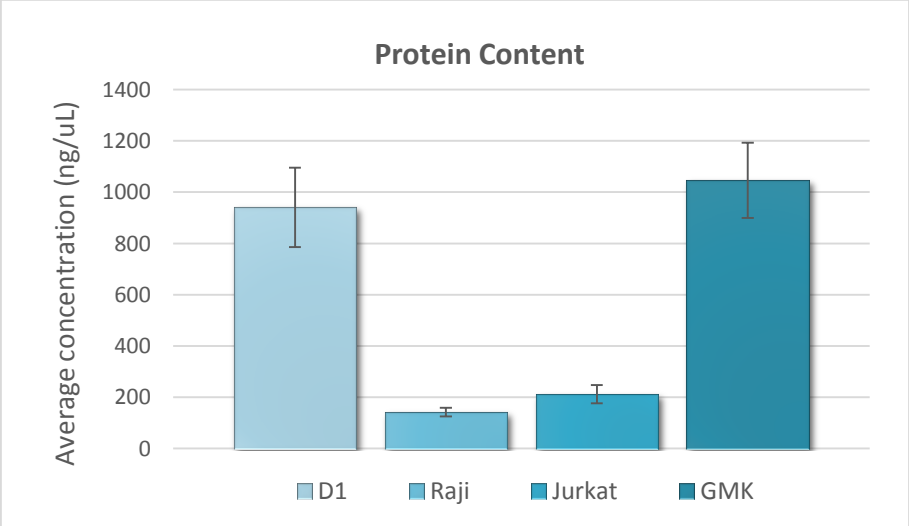

Figure 10 Detected protein content of the NMV suspensions.

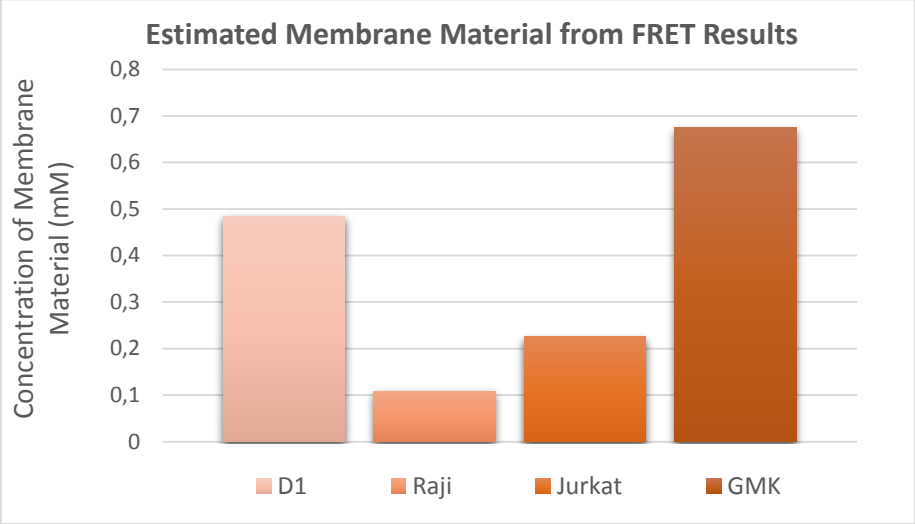

Figure 11 Estimated membrane material calculated from FRET results for the different NMV suspensions.

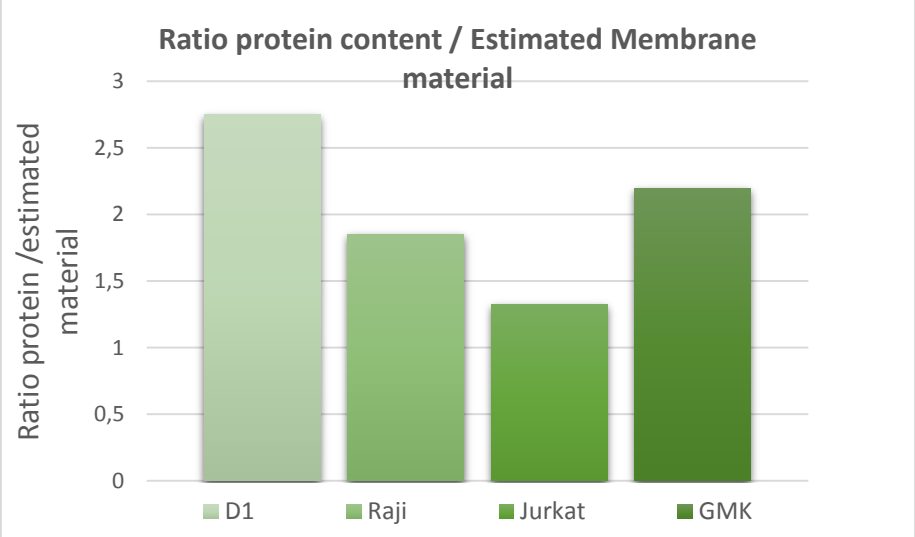

Figure 12 Ratio of protein divided by estimated membrane material.

The total protein concentration and estimated membrane material follows an expected trend with a high protein concentration in the samples of higher membrane material. The results in figure 12 suggest that D1 cells have the highest protein content in their membrane after the production of NMVs. In contrast, Jurkat T cells have the lowest content of protein in the vesicular material.

The amount of vesicle material determined by the FRET assay represents a means to compare the different native materials rather than an absolute quantification. Indeed, the estimate is based on several assumptions. First of all, the complex material composition of the native membrane is neglected, and synthetic POPC lipid vesicles are used as standards. The estimate also assumes that the FRET conditions are optimal, and all membrane material mixes, an assumption that might be inaccurate depending on the vesicle composition and on their fuosogenecity. Nevertheless, these values provide a comparison of the relative material concentration of the native membrane materials, as previously mentioned, which facilitates further analysis and comparison between NMV types and batches.

5.2 CHARACTERIZATION OF FUSION POTENTIAL OF NATIVE MEMBRANE VESICLES

After creating NMVs from the different cells, FRET was used to investigate the potential of the vesicles to fuse with synthetic lipids by sonication, to form hybrid vesicles. The ability to mix by sonication was tested by looking at the fluorescence intensity over different wavelengths where the ratio between the two peaks (530/590nm) provides an indication of the degree of mixing of the two components: The higher the ratio the better the mixing as this results from a higher emission from the donor FRET probe, and therefore a higher separation between the acceptor and donor molecules due to mixing with unlabeled membrane material. Different conditions for sonication were tested during FRET experiments for each NMV type. The variables investigated were time and temperature of sonication.

The resulting FRET signals can be seen in figures 13-15 as the average fluorescence intensity detected for different wavelengths.

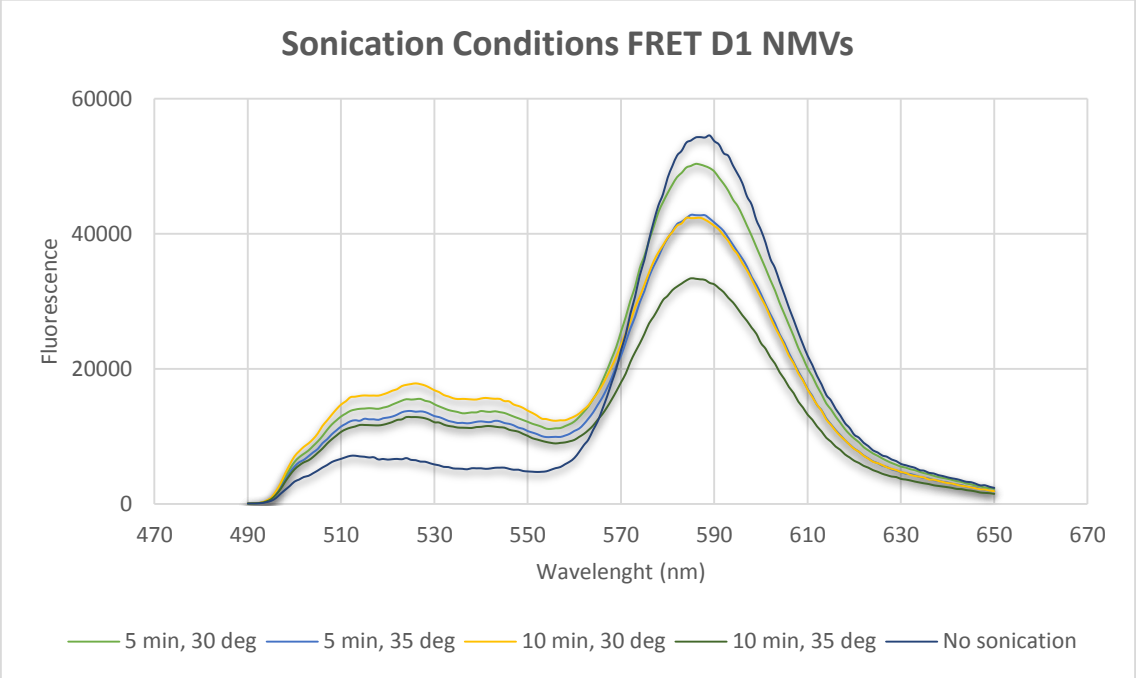

Figure 13 FRET emission from D1 NMV hybrids, labeled with NBD and rhodamine, after different sonication treatments.

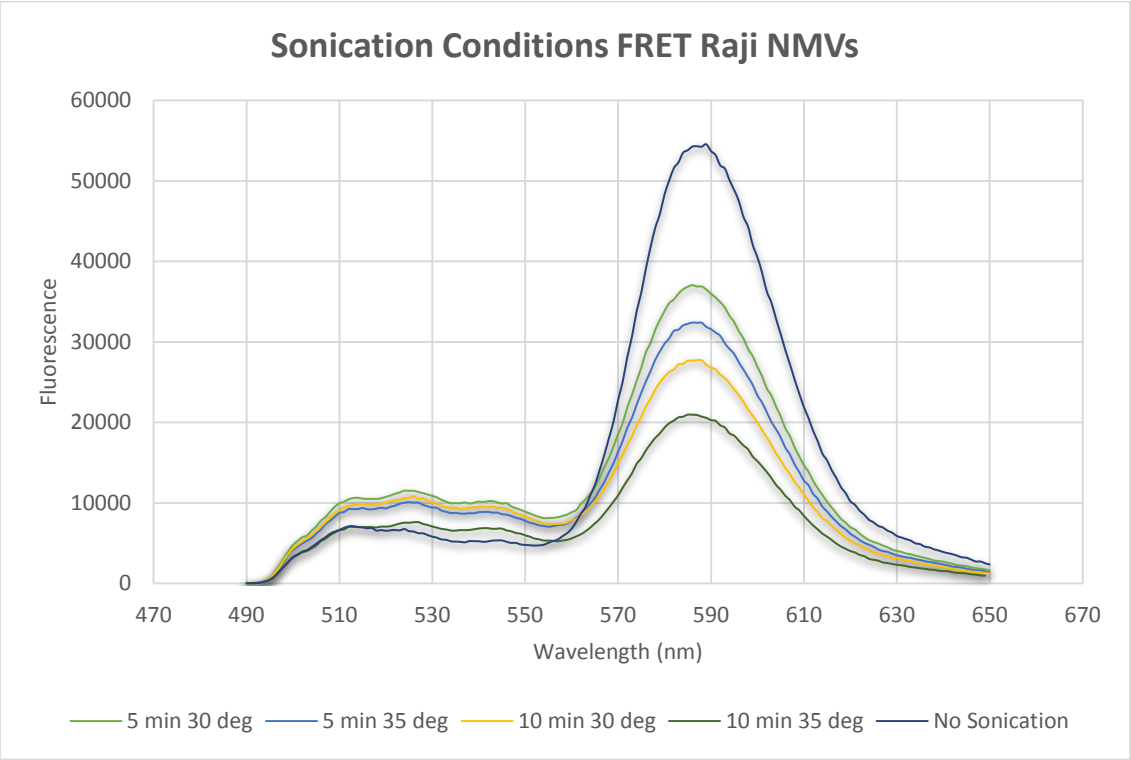

Figure 14 FRET emission from Raji NMV hybrids, labeled with NBD and rhodamine, after different sonication treatments.

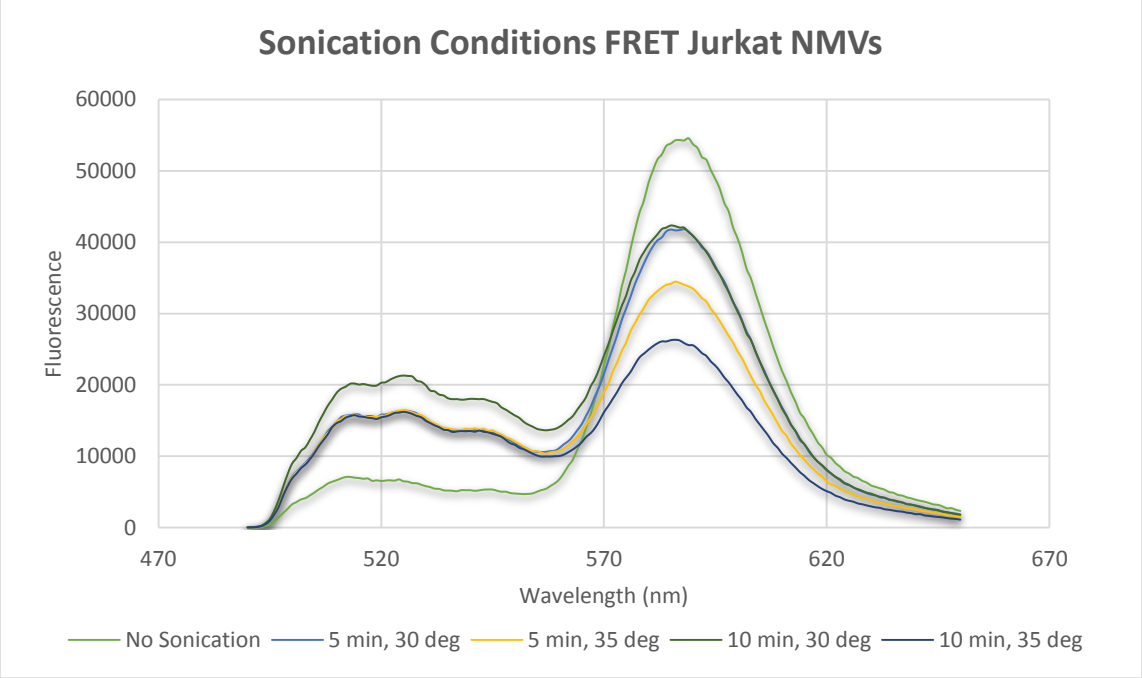

Figure 15 FRET emission from Jurkat NMV hybrids, labeled with NBD and rhodamine, after different sonication treatments.

The ratios between the peaks (530/590 nm) were calculated to compare the resulting FRET of each sonication condition as can be seen in Figure 16. (The numerical values can be found in supporting information, chapter 9). The highest mixing ratio for D1 NMVs and Raji hybrids is obtained after 10 minutes of sonication at 30 °C while the Jurkat hybrids appeared to require more extreme sonication conditions as the highest ratio was obtained for the sonication conditions of 10 minutes and 35 degrees Celsius. All following experiments were therefore performed using the conditions of 30°C for 10 minutes for D1 and Raji NMVs, but the higher temperature of 35°C for the Jurkat NMVs.

Furthermore, as shown in figure 16, our results on immune cells were further compared with the ones obtained on an epithelial cell line using NMVs from Green Monkey Kidney (GMK) (data provided by master's thesis student Eneas Schmidt). The results show that sufficiently high temperature is of importance for the fusion of NMV vesicles, as seen in the GMK graph, where 30°C produced better fusion of the vesicles than 20°C. The other experiments with the other NMV types reveal that time of sonication treatment had a bigger importance for the fusion ability than the temperature. In these experiments the temperatures were higher, and the compared time periods were shorter.

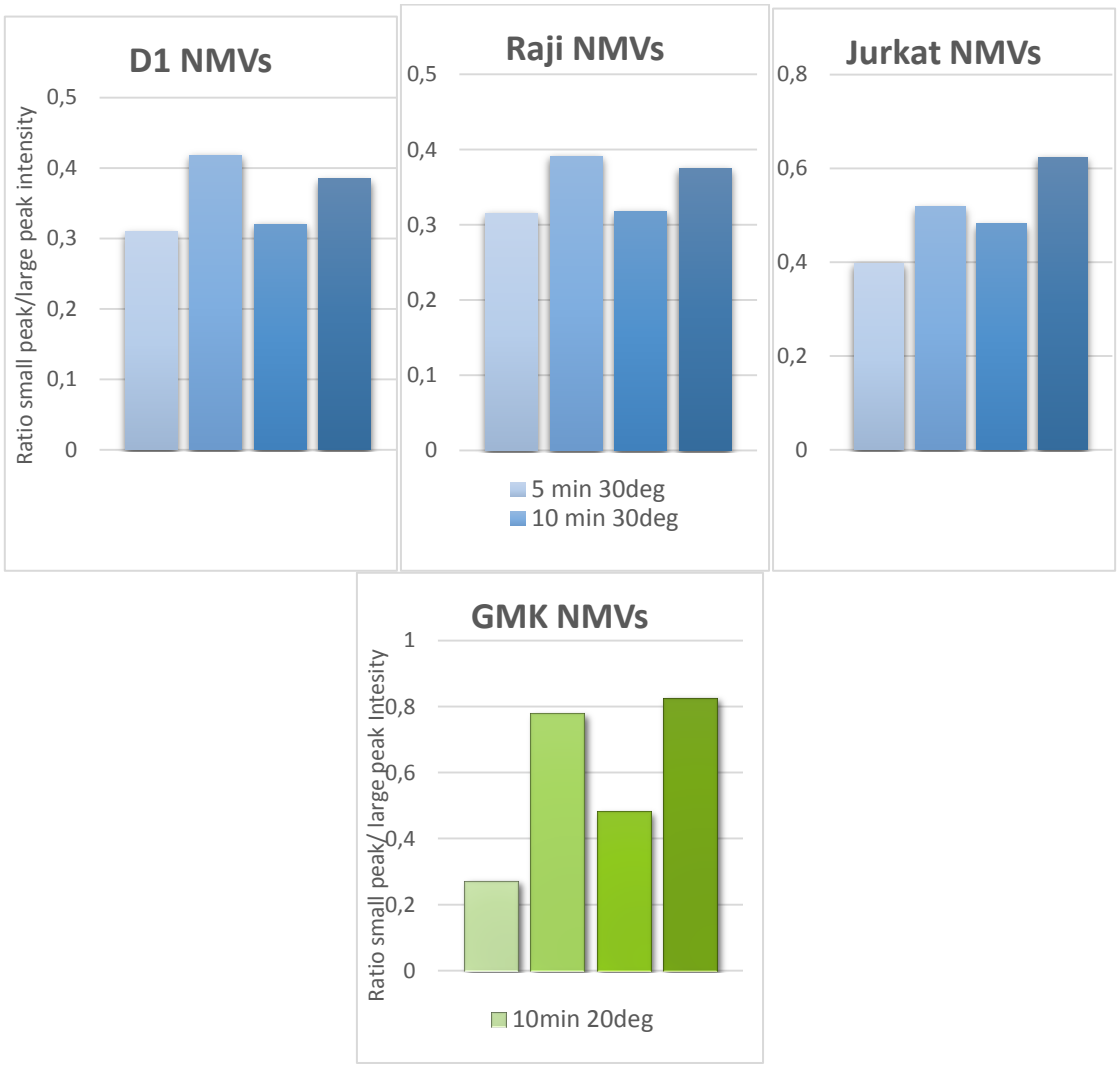

Figure 16 Mixing of vesicles in FRET assay for different sonication conditions used. Represented as bars for the values of ratios (530/590 nm). Higher bar indicates better mixing of vesicles.

5.3 CHARACTERIZATION OF BILAYERS

5.3.1 Bilayer formation

To investigate the influence of the amount of native material on bilayer formation and hence to determine the optimal parameters for bilayer formation, bilayers consisting of different ratios of NMVs to PEG_POPC lipids were formed. Small amounts of rhodamine-labelled tracer vesicles were added to the experiment in order to follow bilayer formation under the microscope. Non-ruptured fluorescent vesicles on the substrate were detected and quantified over time for the different NMV types, as shown in figures 17 to 19, as well the number of detected vesicles through the process of SLB formations of each NMV composition can be seen in tables 3 to 5. The percentage of nonruptured vesicles, as shown in the tables 3 to 5 provides a good representation of the success of the SLB formation, as further described below.

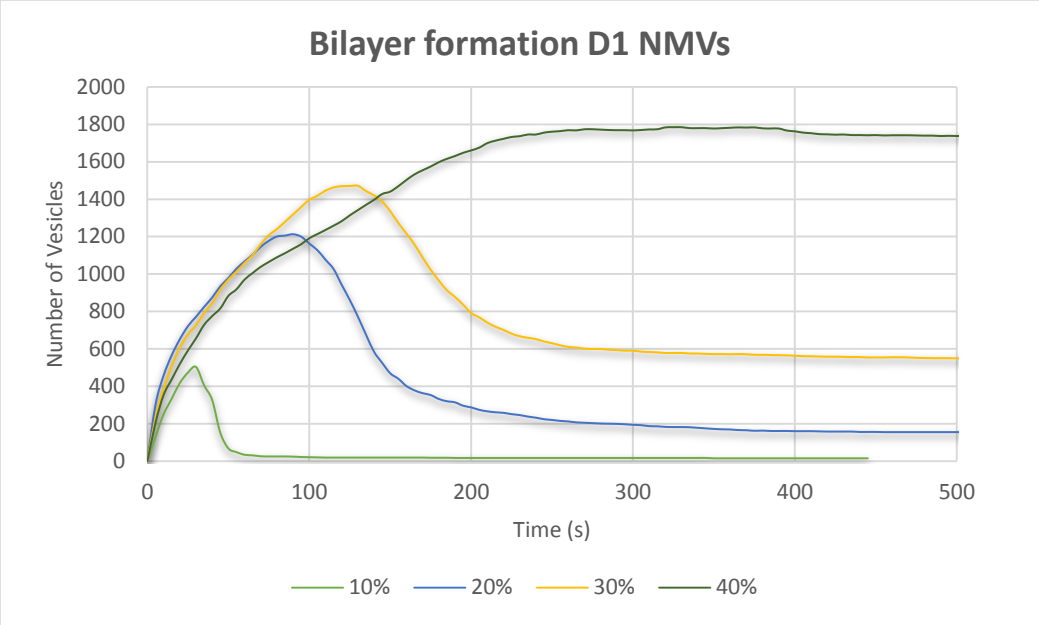

Figure 17 Number of detected non-ruptured vesicles on the substrate surface over time, for varied compositions of D1 NMV hybrid vesicles.

Table 3 Bilayer formation of D1 NMVs

NMVs (vol%)	Max. amount	Average Final	Non-ruptured (%)
10	503	16,11	3,2
20	1212	152,56	13
30	1471	525,05	36
40	1784	1668,69	94

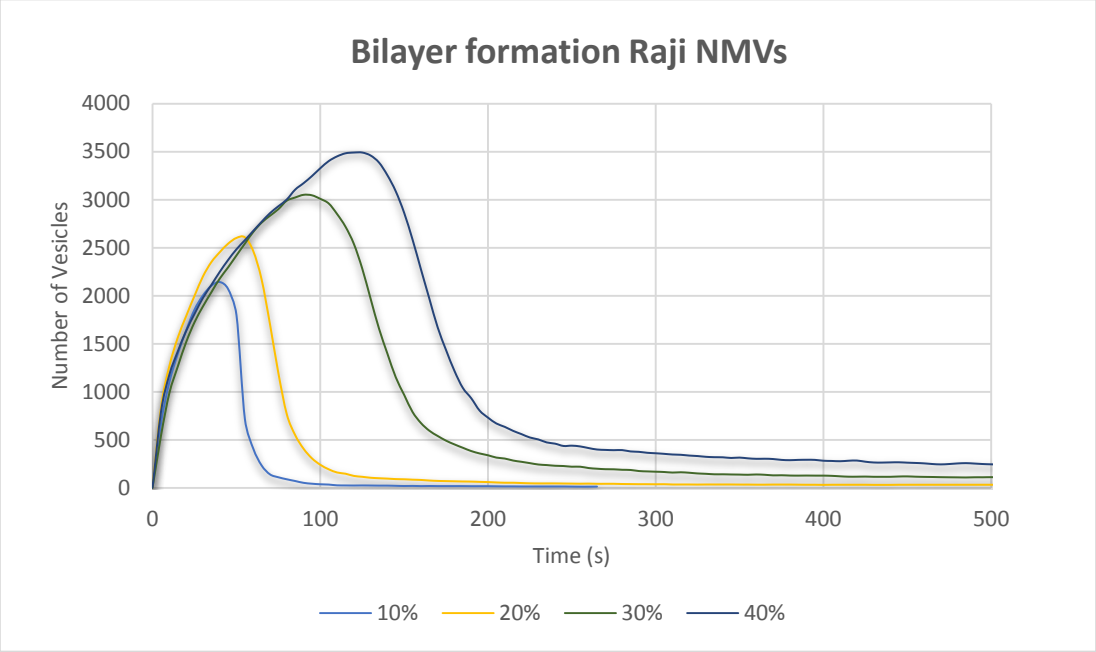

Figure 18 Number of detected non-ruptured vesicles on the substrate surface over time, for varied compositions of Raji NMV hybrid vesicles

Table 4 Bilayer formation of Raji NMVs

NMVs (vol%)	Max. Amount	Average Final	Non-ruptured (%)
0	4505	17,35	0,39
10	2143	14,27	0,67
20	2608	31,83	1,22
30	3051	92,91	3,05
40	3491	242,35	6,94

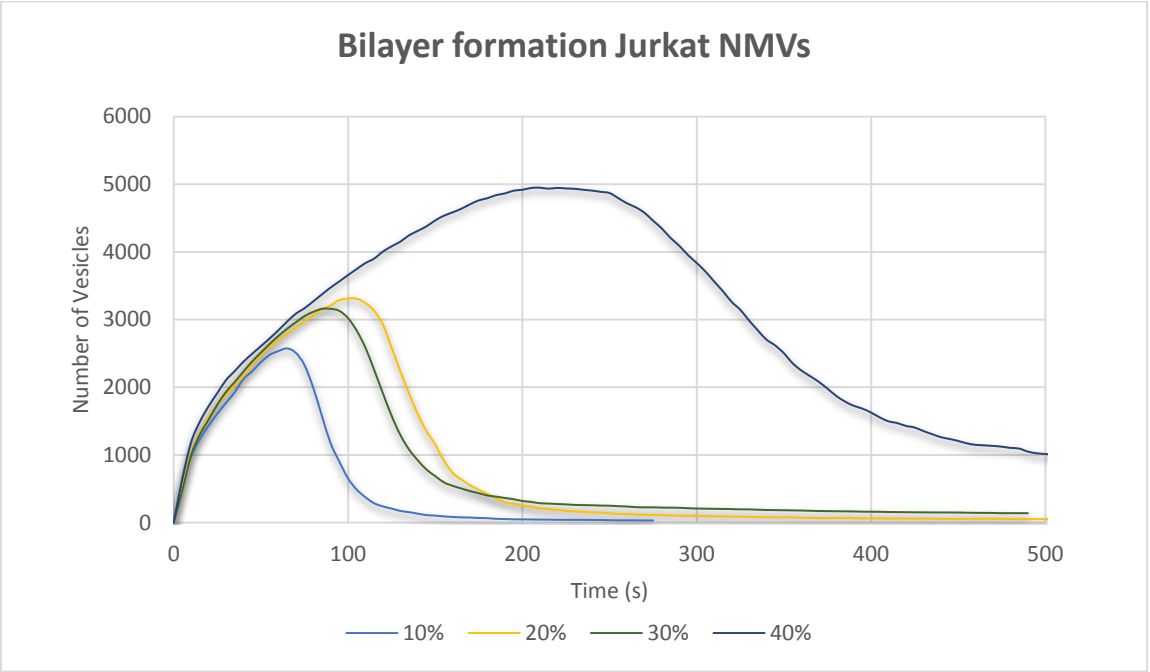

Figure 19 Number of detected non-ruptured vesicles on the substrate surface over time, for varied compositions of Jurkat NMV hybrid vesicles

Table 5 Bilayer formation of Jurkat NMVs

NMVs (vol%)	Max. Amount	Average Final	Non-ruptured (%)
0	3136	271	8,64
10	2574	38,77	1,51
20	3310	50,44	1,52
30	3159	146,38	4,63
40	4948	463,63	9,37

In the graphs it can be seen that the number of vesicles detected is initially rising as more vesicles land on the surface. When a critical vesicle surface coverage is reached, the sudden decrease in number of detected vesicles is associated with the process of rupture and bilayer formation, since the vesicles are not detected after rupture. The rupture events, which starts to occur at critical vesicle concentration, initiates more ruptures, thereby catalyzing the bilayer formation process. From this data, the time until bilayer formation can be estimated for each composition. Additionally, these experiments allow for a relative comparison of the amount of PEG-POPC material needed to induce rupture of NMV–containing hybrid vesicles.

As seen in the graphs, bilayer formation was observed in compositions of the 10-30%vol NMV for all NMV types, and also for 40%vol for the Raji and Jurkat NMVs, seen in figure 18 and 19. It appeared that the rupture events take place sooner for hybrid vesicles containing lower levels of native material. Furthermore, no major rupture event takes place for the 40%vol D1 NMV hybrid vesicles, indicating that for this composition no SLB was formed. The percentage of nonruptured vesicles is very high for the D1 40%vol

composition, as seen in table 3, further indicating a lack of bilayer formation. Based on these results, further experiments using D1 NMV for bilayer formation are done using 20% and 30% mixtures. Bilayers were formed for all tested concentrations of Raji NMVs in the hybrid vesicles. Based on these results, further experiments using Raji NMVs in the formation of bilayers are done using 30% and 40% mixtures. Bilayers were formed for all tested concentrations of Jurkat NMVs in the hybrid vesicles, but not as successfully for the 40% composition, as no specific rupture event is observed. Based on these results, further experiments using Jurkat NMVs in the formation of bilayers are done using 30% mixtures. This is to maximize the presence of the native membrane components of the native membrane material while still permitting SLB formation.

So far, the results have been described by reporting the amounts of native material in volume percent. While such an approach is useful from a practical point of view, it doesn't allow for a comparison of the samples. Therefore, the amount of membrane material estimated from FRET results (see figure 11) was used to provide a quantitative estimate of the amount of membrane material contained in each sample and the amount of non-ruptured vesicles as function of NMV material content is shown in figure 20.

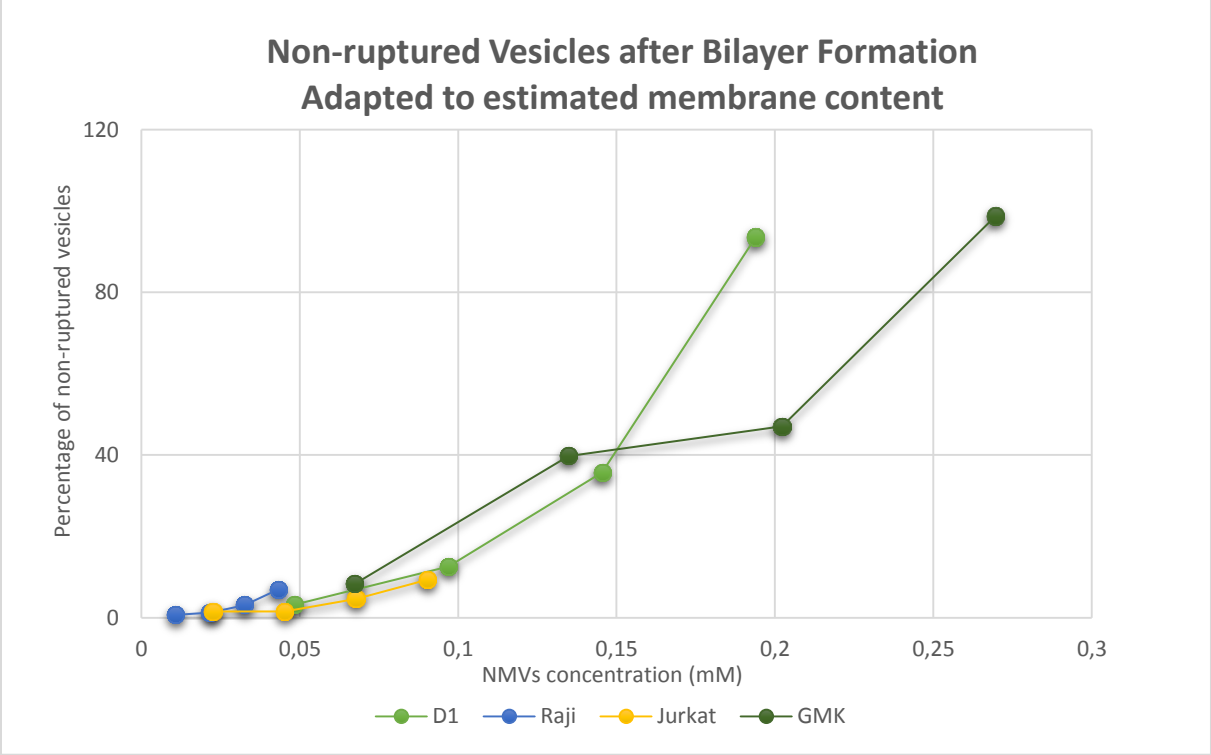

Figure 20 Concentration of NMV material in hybrid vesicle material when adapted to calculated estimated membrane material

This normalization confirms that there is difference between the concentrations of material in the used volumes, which is most likely the cause might be the cause of the difference in abilities for bilayer formation observed for the different samples at the same volume content. D1 NMVs did not form bilayers at the 40%vol composition, which is reasonable since the estimated material concentration in the D1 NMV solution is

approximately twice as high as the 40%vol Jurkat NMV solution, and four times as high as the 40%vol Raji solution. The graph indicates a trend in bilayer formation using NMV hybrids, where NMV concentration, rather the type of NMV material in the hybrid composition is highly relevant for the number of non-ruptured vesicles.

5.3.2 Fluorescence recovery after photo bleaching

To investigate the quality of bilayers formed as well as the mobility of the bilayer components, FRAP was used on bilayers of 20% and 30% D1 NMV hybrids, where the synthetic PEG_POPC vesicles were labeled with rhodamine. The bleaching and the recovery in intensity over time makes it possible to visualize the mobility of the lipids. The recovery as a function of the NMV content can be seen in figures 21 and 22 below, where the bleached spot can be seen, as well as the recovery at two time points.

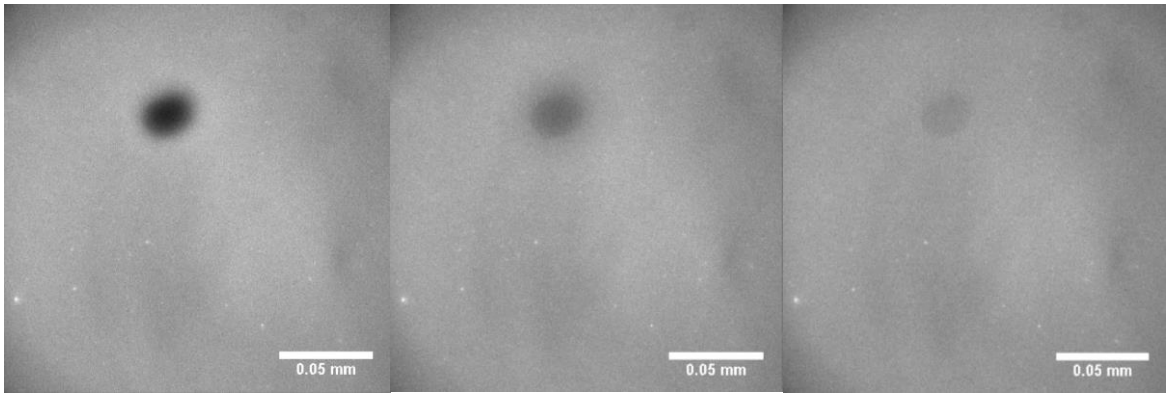

Figure 21 FRAP recovery for 20% NMV hybrid SLB, at times 0, 65 and 600s.

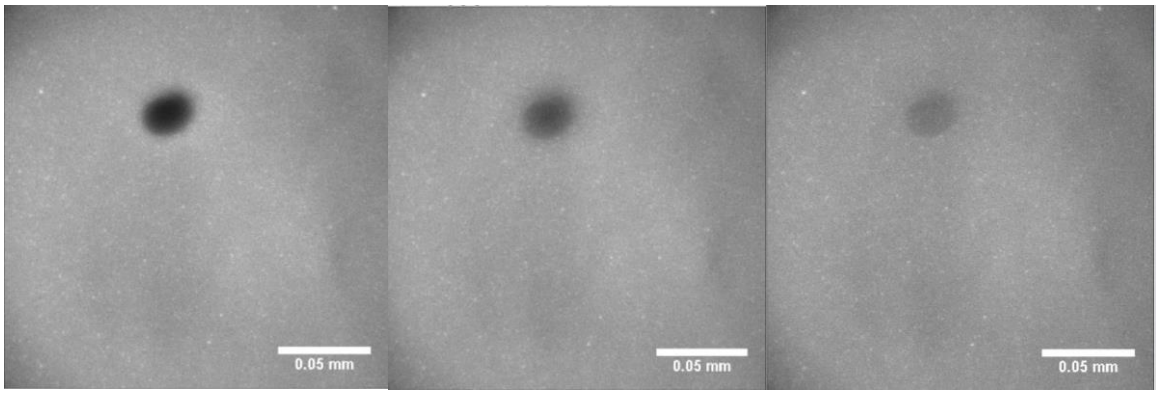

Figure 22 FRAP recovery for 30% NMV hybrid SLB, at frames 0, 65 and 420s.

The calculated values for each recorded FRAP can be seen below in table 6.

Table 6 Diffusion and immobile fraction of the SLBs, with standard deviations.

NMVs Fraction	Diffusion (um^2s^-1)	Immoblie Fraction (%)
0%	1,39 ± 0,0043	0,21 ± 0,18
20%	0,73 ± 0,038	14 ± 0,95

30%	0,35 ± 0,044	24 ± 2,9

From these results it can be seen that the diffusion coefficient decreases as the fraction of native membrane is increased. The NMVs therefore lowers the mobility of the lipids in the bilayer. The immobile fraction increases with the increased native membrane fraction due to the presence of non-ruptured vesicles. This can be seen represented below in figure 23 and 24.

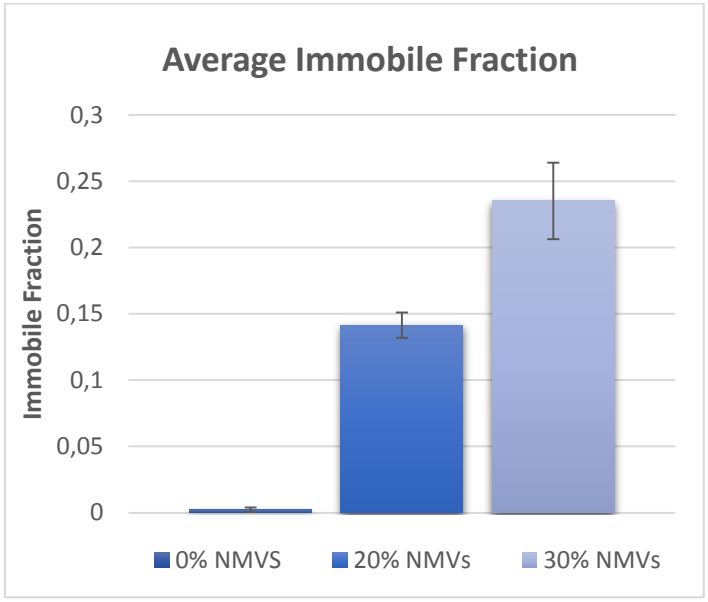

Figure 23 Average immobile fraction of the different SLB compositions, with standard deviation.

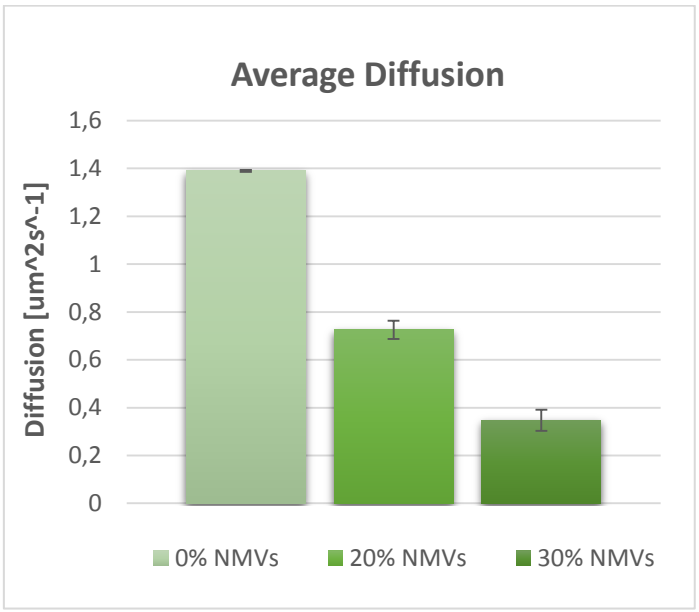

Figure 24 Average diffusion of the different SLB compositions, with standard deviation.

5.4 FLUORESCENT RECOVERY AFTER PHOTOBLEACHING OF MHC TYPE II COMPLEXES

FRAP was performed on SLBs derived from Raji B cell NMVs, where antigen presenting complexes MHC type II were detected using a fluorescent PE labeled anti-human HLA-DR antibody. Below are images from the FRAP experiment, right after bleaching, as well as after a two-hour period.

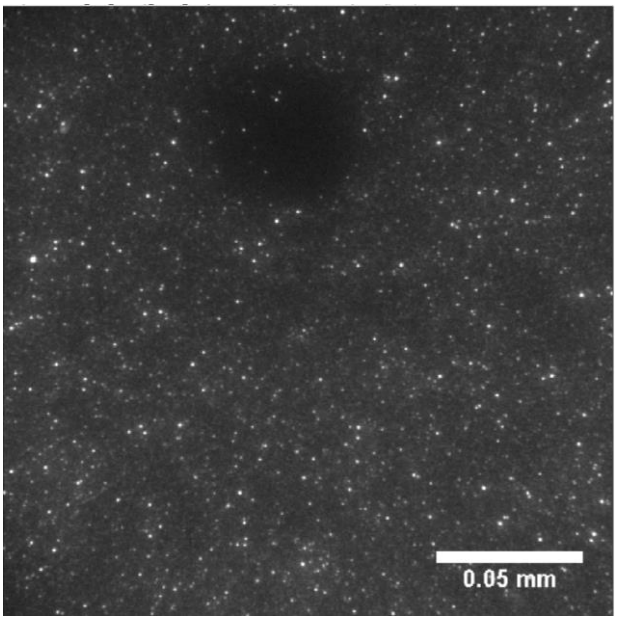

Figure 25 FRAP image of anti-human HLA-DR antibody on Raji derived SLB. Fame 6, directly after bleaching.

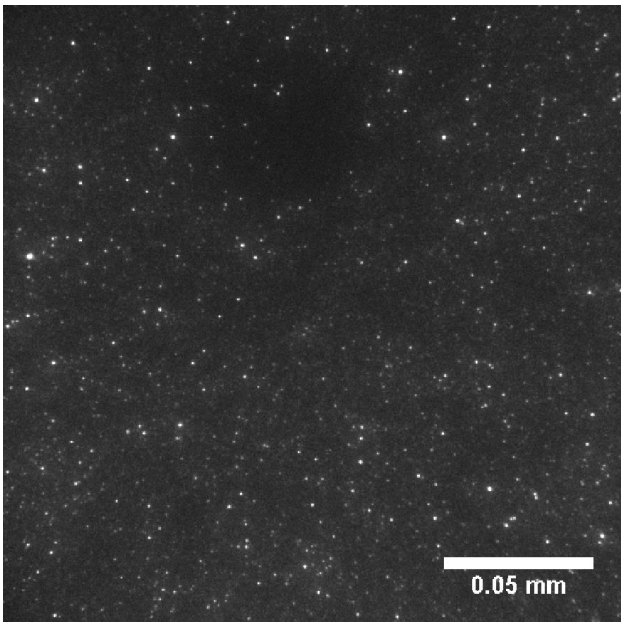

Figure 26 FRAP image of anti-human HLA-DR antibody on Raji derived SLB. Frame 66, 2 h after bleaching.

FRAP analysis resulted in a very low diffusion of 0,0058 [um^2s^-1], but also in a relatively low immobile fraction of 9,67 %. The images showed quite high levels of bleaching throughout the experiment. Visual observation showed evenly spread small dots as well as larger clusters of intensity over the surfaces. As this experiment was performed late in the project period, the experiment has not yet been reproduced, and

no negative control is included. This experiment therefore needs to be repeated and optimized to be further analyzed. Even so, the antibodies label antigen presentation with the MHC type II complex, and gives good intensity in the experiment reported.

5.5 BILAYER-CELL INTERACTIONS

In order to investigate the bilayers biofunctionality and it's potential in promoting cell attachment, Jurkat T cells were incubated on newly formed SLBs consisting of NMV hybrids of Raji cells. The interaction between T-cell and B-cell is the initial step of the formation of an immunological synapse which is to be studied using the developed platform. Raji B lymphocytes carry the antigen presenting MHC type II complex for initiation of the cellular interaction with Jurkat T lymphocytes. To further assess the specificity of cell attachment, cells were also placed and incubated on control surfaces of Jurkat-derived SLBs, pure synthetic PEG_POPC SLBs and pure glass substrate.

Images of the cells on the surfaces were captured after incubation, and after the samples were shaken in order to quantitatively test the attachment of the cells to the surface. Sample images acquired after shaking are visualized below in Figure 27.

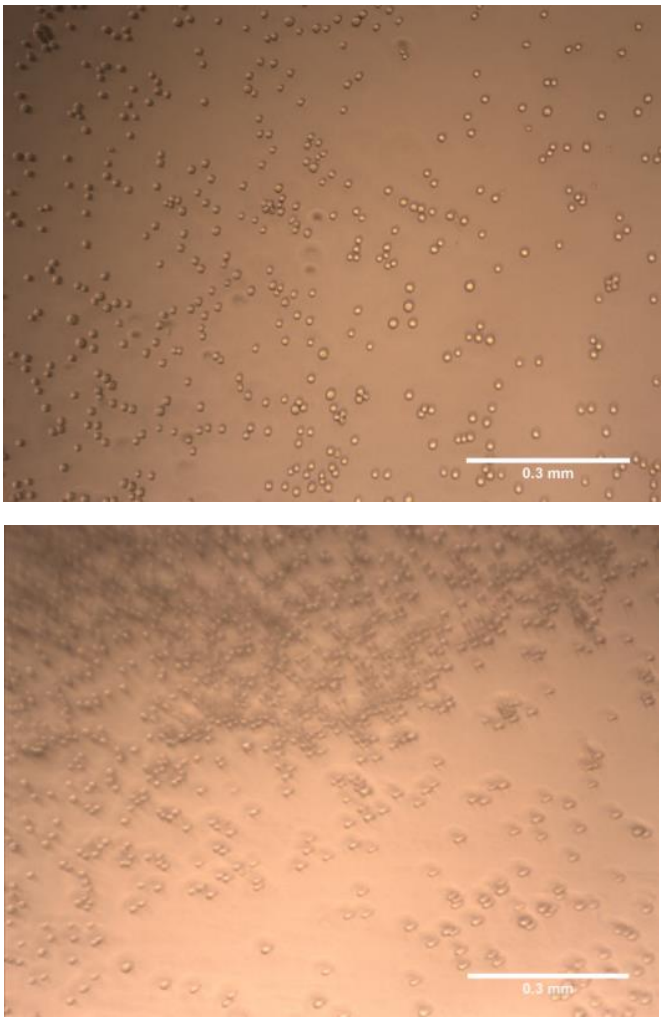

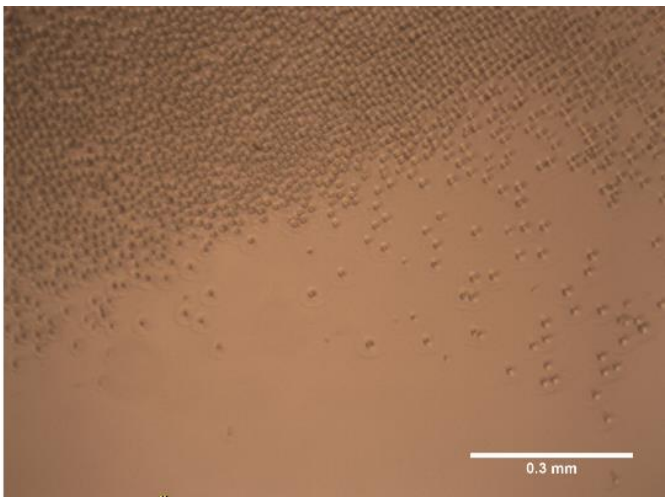

Figure 27 Images after shaking the SLB surfaces with cells. Raji, Jurkat and PEG_ POPC respectively.

As seen in the pictures, T cells were collected in piles from the shaking motion to a higher extent on the control POPC-PEG and glass surfaces This indicates a stronger attachment of cells to the Raji SLBs than to the other surfaces. More images of the cells were captured after the wells were rinsed with medium repeatedly. This can be seen in representative images below.

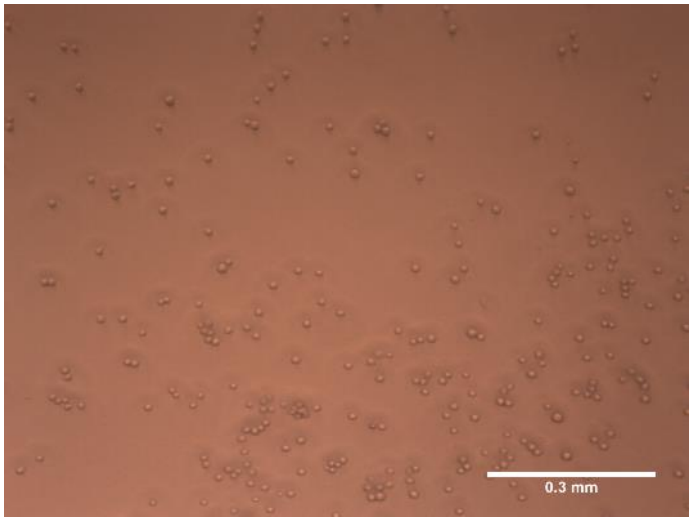

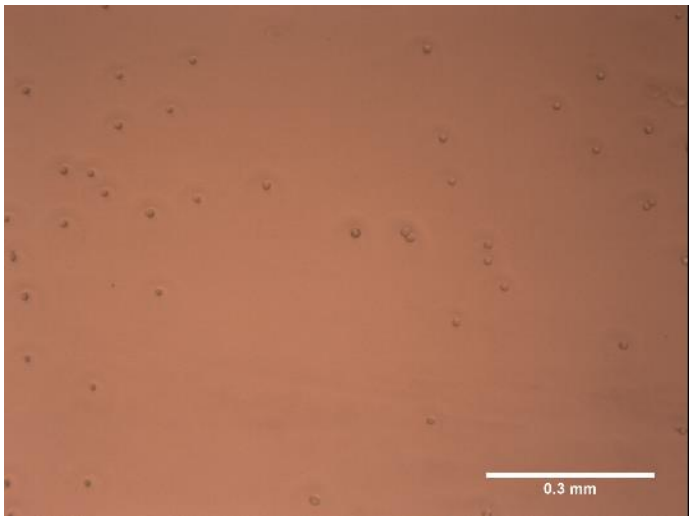

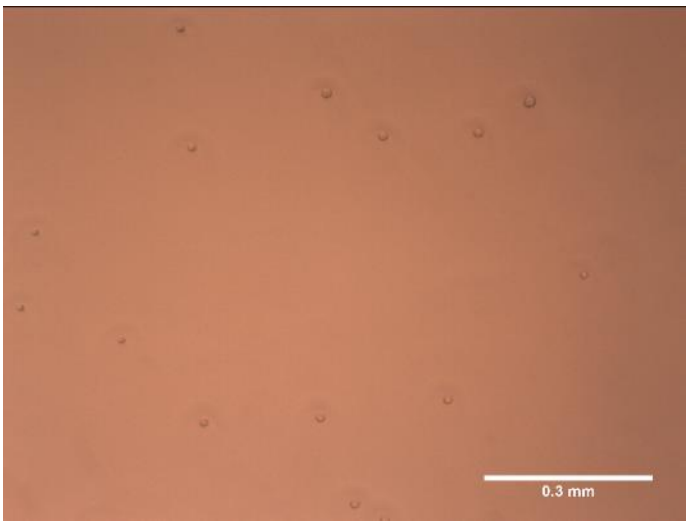

Figure 28 Images after rinsing the SLB surfaces with cells. Raji, Jurkat and PEG_ POPC respectively.

As can be seen in the images, more cells remain on the B cell derived surfaces, which suggests a better attachment of the cells to these SLBs. This is further confirmed after data evaluation (figure 29).

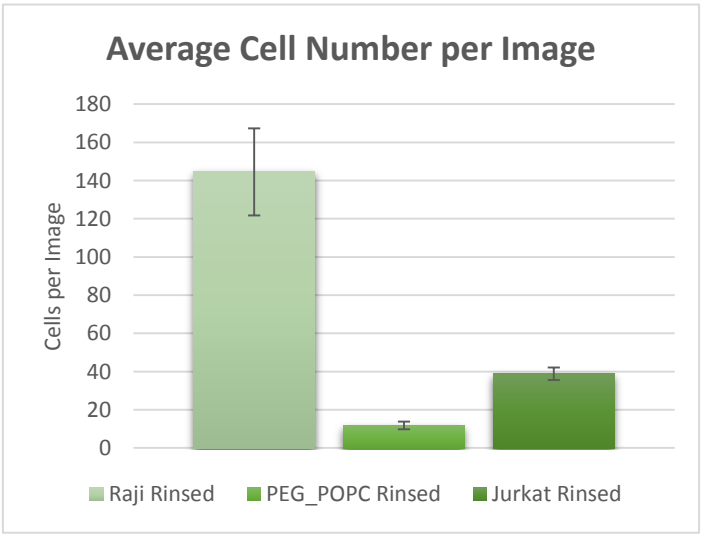

Figure 29 Average numbers of cells counted per image of each SLB type, after rinsing.

These results suggest a stronger attachment of live Jurkat T lymphocytes to SLBs produced from Raji derived NMVs than any of the used control surfaces. This indicates interaction between the T cells and the B cell derived bilayer. Previous experiments performed within this thesis, have shown a similar trend, but the results provided a more clear result with the presented experiment, which was performed with a longer incubation period (1h) than other experiments (30min).

After the SLBs were rinsed, additional images were captured, using a 60x objective. Resulting pictures are presented below.

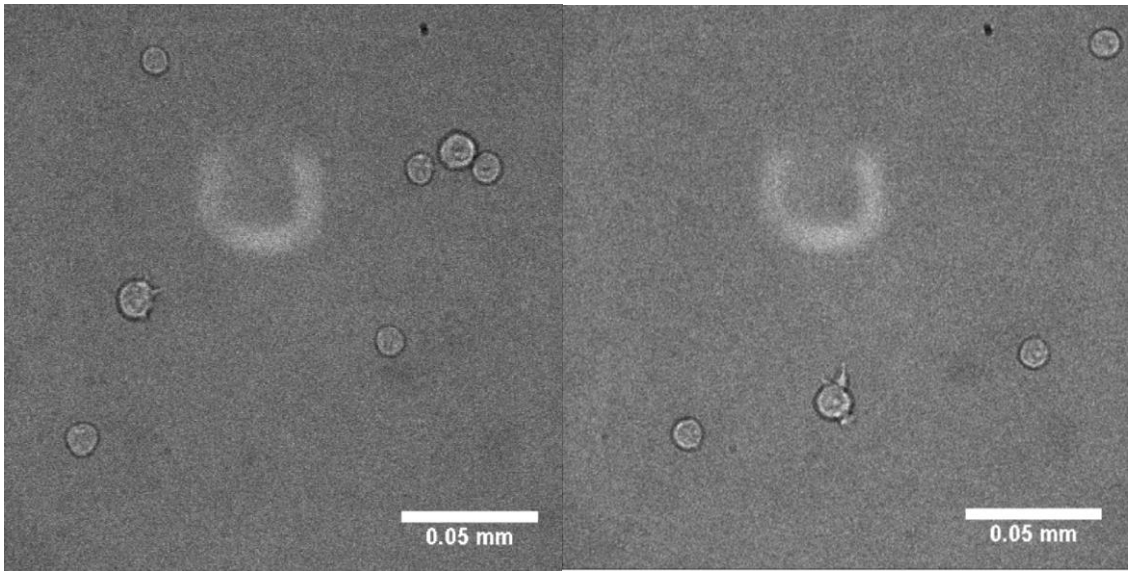

Figure 30 T cells on rinsed Raji.

The round shape of the cells is an indication that they are healthy, as it is the natural shape of the Jurkat cell line. In addition, some cells displayed outgrown extensions on the surfaces. These were mostly observed on the Raji SLBs, but also on the PEG_POPC SLBs.

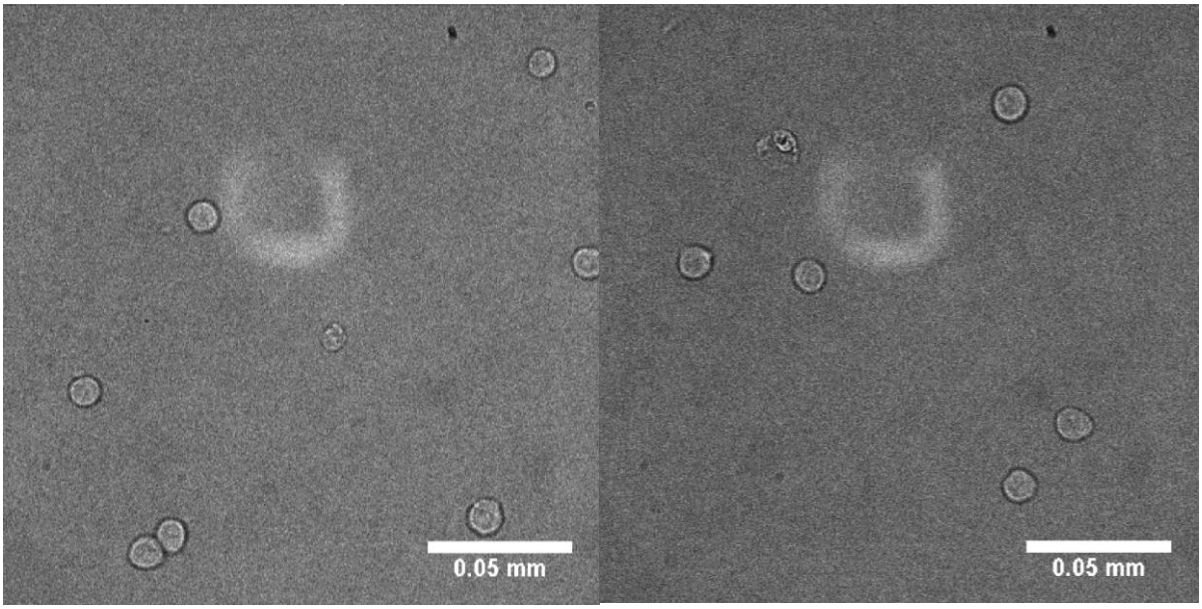

Figure 31 T cells on rinsed Jurkat SLBs.

The T cells on the Jurkat T cell SLB hold their normal round shape, except for a few smaller or misshapen cells.

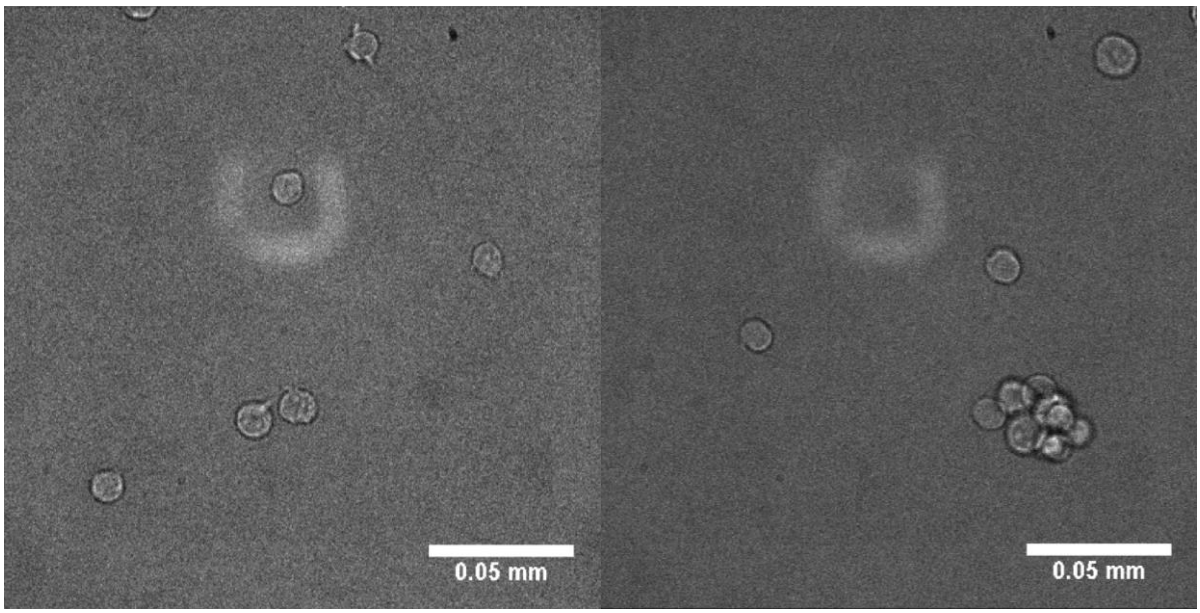

Figure 32 T cells on rinsed PEG_POPC SLB.

Seen on the PEG_POPC SLB were cells with previously mentioned outgrown extensions, and also clustered cells in small piles.

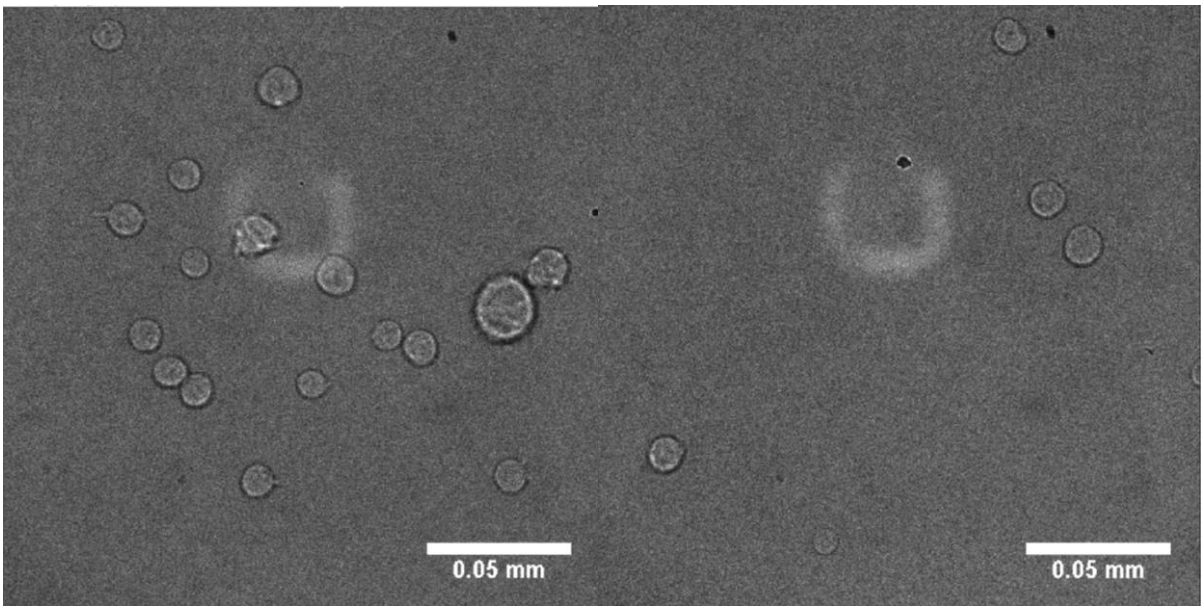

Figure 33 T cells on rinsed glass slide.

Observations of the glass substrate provided the most uneven morphology of the cells, as they varied in size, shape, and level of clustering over the surface.

6 DISCUSSION

This project has been an exploratory project, where the experiments conducted, and hypothesis investigated, have changed continuously throughout the process while new results were interpreted. As a result of this, most results are initial, and the methods developed need optimization and further testing. The results as such are still interesting and hold potential for further interesting experiments.

Throughout the project, SLBs have been successfully produced for all immune cells used. The production procedure of NMVs resulted in a varied concentration of material of the different NMV types yielding bilayers of different content of native material. Nevertheless, the successful formation of bilayers with complex membrane material from the different cell types provides a good foundation for further studies using SLBs for investigating immunological cells.

6.1 CHARACTERIZATION OF NATIVE MEMBRANE VESICLES

In order to characterize the NMVs, the protein, phospholipid and total material content of the NMV suspensions was determined. FRET was further used to investigate the mixing potential of the NMVs using bath sonication and to estimate the membrane material concentration by calibration against POPC. This information was gathered to better understand the requirements for successful fusion of NMV vesicles into hybrid vesicles, as well as to optimize the parameters of SLB formation regarding treatment conditions and composition of the vesicles.

Comparison of sonication conditions for mixing gave a result indicating that the NMVs require higher temperatures for FRET mixing, compared to synthetic vesicles which were shown in previous studies (1) to require lower temperatures in order to fuse than NMVs. This might be directly related to the more complex composition of the NMVs. The NMVs containing larger transmembrane protein complexes, cholesterol rich lipid rafts and gel-phase lipids with higher transition temperatures than POPC which might require more sonication energy to achieve fusion of the membranes. In addition, one can question what impact the sonication procedure has on protein functionality of the native membranes, as the heat and material transfer upon fusion might impact the configuration and folding of proteins. This aspect was not extensively considered in this work but should be further investigated in future experiments by more detailed tests of functionality of the membrane components. Purified proteins that are known to be present and functional in the native membranes could perhaps also be studied to identify changes in configuration at different temperatures and sonication treatments, in order to better predict their functionality in the hybrid vesicles.

6.2 CHARACTERIZATION OF SUPPORTED LIPID BILAYERS

In order to characterize the SLBs, the bilayer formation process was first investigated. In addition, the mobility of lipids of the SLBs, as well as the mobility of the labeled protein complexes was assessed.

6.2.1 Bilayer formation

The results of experiments carried out at different volume ratios of starting NMV material were normalized using the estimated membrane material content calculated from the FRET experiments, making it possible to investigate how the bilayer formation depends on the composition. From figure 20, it was concluded that higher levels of NMV material hinders the bilayer formation, and all types of NMVs that were investigated fall on the same trend. This indicates that it is the amount of native material that determines the rate of bilayer formation rather than the type and the composition of the different cell membranes used. From this trend, a conclusion can be drawn regarding what concentrations of NMVs in a hybrid composition might be optimal when forming SLBs in general, in order to achieve bilayer formation with as high concentration of NMV material as possible. This information can be very useful in future studies of SLBs formed from NMV hybrid compositions.

6.2.2 Detection of membrane components

FRAP was performed on D1 derived SLBs, produced using rhodamine labeled PEG_POPC. This was done to investigate the overall mobility of the molecules of the formed SLBs. As seen in the graphs, there is a clear trend for decreased mobility of the fluorescently labeled lipids with increased NMV concentration. This is consistent with the literature, as the cells contains lipid rafts in their membrane and therefore large amounts of cholesterol. The diffusion coefficient measured in FRAP is relatively insensitive to variations of phospholipid composition, but quite sensitive to introduction of cholesterol which lowers the diffusion. (24) FRAP was also performed to study antibody-labelled MHC class II complexes in Raji derived NMVs. The results show very low diffusion of the labeled complexes, at 0,0058 [um^2s^-1]. This does not fit the values found in literature of diffusion coefficient 0,18-0,22[um^2s^-1] for MHC class II complexes. (25) As the study providing the literature values was performed by observation of the MHC complexes of cells, a very likely cause for the lower diffusion in the SLBs is the interaction with the substrate surface, which hinders movement.

One important issue to consider when detecting the presence and potential functions of membrane components in the constructed SLBs, is that the orientations of the molecules in the membrane are lost through the process of cell homogenization, sonication and SLB formation (1). This might have an impact on the properties of the membrane, as the more complex biomolecular reactions might be dependent on the orientation of the combined components. In spite of this limitation, the constructed model is still closer to the native situation it aims to mimic, compared to the synthetic constructions with only a few native components, described in the theoretical background. Nevertheless, the issue should still be considered in further use of the developed model. The alternate approach described in the background (18), and using cell blebs, rupturing with a "parachute" mechanism that retains the orientation of the bilayer might be considered if this is deemed an important issue. The difference in the protocols gives different results as the bleb-based method does not utilize sonication, and therefore does not disrupt the orientation by mixing up the lipid material. Another point regarding the blebbing procedure, is that the formed SLBs might not be as representative of normal native membrane composition as the SLBs produced with the NMV-procedure. This, because the blebbing is induced by subjecting the cells to stress, which might induce reactions

other than the blebbing and affect the biomolecular composition of the blebs themselves.

6.3 BILAYER - LIVE CELL INTERACTIONS

The experiments conducted using live Jurkat T cells on Raji derived SLBs show a clear result of better attachment of the cells to the Raji SLBs than the other surfaces. Attachment was also shown to be time-dependent with a stronger attachment when the cell incubation time was increased from 30 minutes to 60 minutes. As the immunological synapse takes place over several hours, it is likely that the longer incubation time increases the adhesion of the cells to the bilayer.

An interesting question to consider for further experiments of adhesion of live cells to SLB surfaces is the effect of the cushioning PEG structure. It is, as previously described, added to the synthetic vesicles to suspend the membrane over the substrate surface and enable movement of larger transmembrane complexes. As the formation of the immunological synapse is heavily dependent on the stearic hindrance of molecules in the kinetic segregation model, in order to form the SMAC bullseye (6), introduction of large structures might affect the time required for adhesion. As the large PEG cushions might need to move/be pushed out of the area of the synapse, the formation might be delayed by the rate of diffusion of the hindering PEG structures.

7 CONCLUSIONS

The conclusions from this master's thesis are described below in summarized points.

- Different vesicles require different conditions of sonication to achieve mixing with synthetic lipid vesicles. Specifically, in this project, it has been observed that NMVs require higher temperature to achieve mixing with synthetic vesicles compared to synthetic vesicle types.
- Successful SLBs formation was reported for all cell types tested. This shows that the procedure used to produce SLBs is versatile and might be useful for studying a variety of cell types, in addition to the cells of the immune system.
- Higher amounts of NMV material in the hybrid composition lower the fluidity of the SLB. The more complex composition of native membranes lowers the mobility of the lipids of the SLB as they hinder movement with large protein formations.
- Initial results suggest that membrane function is preserved in the SLBs (T cells on SLBs). This aspect needs however to be further investigated for confirmation-

8 REFERENCES

1. *Preserved Transmembrane Protein Mobility in Polymer-Supported Lipid Bilayers Derived from Cell Membranes.* **Pace, Hudson, et al.** Gothenburg : American Chemical Society, 2015, Vol. 87.

2. **Alberts, Bruce, et al.** *Molecular Biology of the Cell, Sixth Edition.* New York : Garland Publishing Inc, 2014. 9780815344643.

3. **Sompayrac, Lauren.** *How the Immune System Works.* Singapore : John Wiley & Sons, Ltd, 2016. 978-1-118-99777-2.

4. *T-cell-antigen recognition and the immunological synapse.* **Huppa, Johannes B. and Davis, Mark M. .** s.l. : Nature Reviews Immunology, 2003, Vol. 3. 1474-1733.

5. *The Immunological Synapse.* **Bromley, Shannon, et al.** s.l. : Annual Reviews Immunology, 2001, Vol. 19.

6. *Initiation of T cell signaling by CD45 segregation at 'close contacts'.* **Chang, Veronica, et al.** s.l. : Nature Immunology, 2016, Vol. 17.

7. *Supported lipid bilayers for the generation of dynamic cell-material interfaces.* **van Weerd, Jasper, Karperien, Marcel and Jonkheijm, Pascal.** Twente : Advanced Healthcare Materials, 2015, Vol. 4.

8. *Supported planar bilayers in studies on immune cell adhesion and communication.* **Groves, Jay T and Dustin, Michael L.** Berkeley : Journal of Immunological Methods, 2003, Vol. 278.

9. *Formation of Solid-supported Lipid Bilayers: An Integrated View.* **Richter, Ralf P, Berat, Remi and Brisson, Alain R.** Pessac Cedex : American Chemical Society, 2006, Vol. 22.

10. *From biological membranes to biomimetic model.* **Eeman, Marc and Deleu, Magali .** 4, Gembloux : Biotechnologie, Agronomie, Société et Environnement, 2009, Vol. 14. 1370-6233.

11. *Specific antibody-dependent interactions between macrophages.* **HAFEMAN, DEAN, VON TSCHARNER, VINZENZ and MCCONNELL, HARDEN.** 7, Stanford : Proceedings of the National Academy of Sciences, 1981, Vol. 78.

12. *Binding of immunogenic peptides to Ia histocompatibility molecules.* **Babbitt, BP, et al.** s.l. : Nature, 1985, Vol. 317.

13. *Architecture and function of membrane proteins in planar supported bilayers: a study with photosynthetic reaction centers.* **Salafsky, J, Groves, J and Boxer, SG.** 47, s.l. : Biochemistry, 1996, Vol. 35.

14. *Identification of self through two-dimensional chemistry and synapses.* **Dustin , ML, et al.** s.l. : Annual Review of Cell and Developmental Biology, 2001, Vol. 17.

15. *A novel adaptor protein orchestrates receptor patterning and cytoskeletal polarity in T-cell contacts.* **Dustin, ML, et al.** 5, s.l. : Cell, 1998, Vol. 94.

16. *Three-dimensional segregation of supramolecular activation clusters in T cells.* **Monks, CR, et al.** 6697, s.l. : Nature, 1998, Vol. 395.

17. *Supported bilayers at the vanguard of immune cell activation studies.* **Dustin, Michael L.** 1, s.l. : Journal of Structural Biology, 2009, Vol. 168.

18. *Membrane Protein Mobility and Orientation Preserved in Supported Bilayers Created Directly from Cell Plasma Membrane Blebs.* **Richards, Mark, et al.** 12, New York : Langmuir, 2016, Vol. 32.

19. *Total Internal Reflection Fluorescence Microscopy in Cell Biology.* **Axelrod, Daniel.** Michigan : Munksgaard International Publishers, 2001. 1398-9219.

20. *Fluorescence Recovery after Photobleaching in material and life sciences: putting theory into practice.* **Loren, Niklas, et al.** Gothenburg : Quarterly Reviews of Biophysics, 2015, Vol. 48.

21. *Fluorescence Resonance Energy Transfer.* **Sondén, Arvid.** Gothenburg : Sahlgrenska Academy, 2008.

22. *Fluorescence Resonance Energy Transfer (FRET) Microscopy - Introductory Concepts.* **Center, Olympus Microscopy Resource.** s.l. : Microscopy Resource Center, 2016.

23. **Technical Reference Library .** *The Molecular Probes Handbook NBD–Rhodamine Energy Transfer.* s.l. : Thermo Fisher Scientific, 2010.

24. *Lateral diffusion in planar lipid bilayers: a fluorescence recovery after photobleaching investigation of its modulation by lipid composition, cholesterol, or alamethicin content and divalent cations.* **Ladha, S, et al.** 3, s.l. : Biophysical Journal, 1996, Vol. 71.

25. *Translational Diffusion of Individual Class II MHC Membrane Proteins in Cells.* **Vrljic, Marija, et al.** 5, s.l. : Biophysical Journal, 2002, Vol. 83.

26. *Supported bilayers at the vanguard of immune cell acativation studies.* **Dustin, Michael L.** 1, s.l. : Journal of Structural Biology, 2009, Vol. 168.

9 SUPPORTING INFORMATION

Table 7 Peak ratios of different sonication conditions.

Sonication Condition D1 NMVs	**Average Ratio (530/590nm)**
5 min 30 deg	0,309169
5 min 35 deg	0,32025
10 min 30 deg	0,417976
10 min 35 deg	0,384464
Sonication conditions Raji NMVs	
no sonication	0,094196
5 min 30 deg	0,315635
10 min 30 deg	0,39131
5 min 35 deg	0,317891
10 min 35 deg	0,375615
Sonication conditions Jurkat NMVs	
no sonication	0,116205
5 min 30 deg	0,39734
10 min 30 deg	0,517661
5 min 35 deg	0,481816
10 min 35 deg	0,623541